*J Physiol* 590.4 (2012) pp 855–873



The Journal of Physiology

# Optogenetic activation of LiGluR-expressing astrocytes evokes anion channel-mediated glutamate release

Dongdong Li[1], Karine Hérault[1], Ehud Y. Isacoff[2], Martin Oheim[1] and Nicole Ropert[1]

[1] *INSERM U603, CNRS UMR 8154, Laboratoire de Neurophysiologie et Nouvelles Microscopies, 45 rue des Saints Pères, Paris, F-75006 France*
[2] *Department of Molecular and Cell Biology and Helen Wills Neuroscience Institute, University of California, Berkeley, CA 94720, USA*

**Non-technical summary** $Ca^{2+}$ increases in astrocytes have been suggested to trigger the release of neuroactive compounds called gliotransmitters. To study the mechanism of gliotransmitter release, it is desirable to have a method able to selectively and reproducibly evoke $Ca^{2+}$ increases in astrocytes. Here, we show that the optogenetic tool the light-gated glutamate receptor 6 (LiGluR) reproducibly evokes $Ca^{2+}$ rises in cultured astrocytes. Combining LiGluR photoactivation and evanescent-field $Ca^{2+}$ imaging, we explored the cellular mechanism of gliotransmitter release from astrocytes in an all-optical manner. The results suggest that high $Ca^{2+}$ in astrocytes triggers the release of glutamate via anion channels rather than vesicular exocytosis.

**Abstract** Increases in astrocyte $Ca^{2+}$ have been suggested to evoke gliotransmitter release, however, the mechanism of release, the identity of such transmitter(s), and even whether and when such release occurs, are controversial, largely due to the lack of a method for selective and reproducible stimulation of electrically silent astrocytes. Here we show that photoactivation of the light-gated $Ca^{2+}$-permeable ionotropic GluR6 glutamate receptor (LiGluR), and to a lesser extent the new $Ca^{2+}$-translocating channelrhodopsin CatCh, evokes more reliable $Ca^{2+}$ elevation than the mutant channelrhodopsin 2, ChR2(H134R) in cultured cortical astrocytes. We used evanescent-field excitation for near-membrane $Ca^{2+}$ imaging, and epifluorescence to activate and inactivate LiGluR. By alternating activation and inactivation light pulses, the LiGluR-evoked $Ca^{2+}$ rises could be graded in amplitude and duration. The optical stimulation of LiGluR-expressing astrocytes evoked probabilistic glutamate-mediated signalling to adjacent LiGluR-non-expressing astrocytes. This astrocyte-to-astrocyte signalling was insensitive to the inactivation of vesicular release, hemichannels and glutamate-transporters, and sensitive to anion channel blockers. Our results show that LiGluR is a powerful tool to selectively and reproducibly activate astrocytes.

(Received 24 August 2011; accepted after revision 4 January 2012; first published online 4 January 2012)
**Corresponding author** N. Ropert and D. Li: INSERM U603, CNRS UMR 8154, Laboratoire de Neurophysiologie et Nouvelles Microscopies, 45 rue des Saints Pères, Paris, F-75006 France. Email: nicole.ropert@parisdescartes.fr and dongdong.li@parisdescartes.fr

**Abbreviations** CatCh, $Ca^{2+}$ translocating channelrhodopsin; ChR2, channelrhodopsin 2; EPI, epifluorescence; ER, endoplasmic reticulum; FWHM, full-width at half-maximum; GFAP, glial fibrillary acidic protein; LiGluR, light-gated glutamate receptor 6; MAG, maleimide-azobenzene-glutamate; ROI, region of interest; SIC, slow inward current; TeTx, tetanus toxin; TIRF(M), total internal reflection fluorescence (microscopy); VGCC, voltage-gated calcium channel.



DOI: 10.1113/jphysiol.2011.219345

## Introduction

Electrically non-excitable astrocytes respond to neurotransmitters with $Ca^{2+}$ elevations (Agulhon *et al.* 2008) that have been suggested to trigger the release of neuroactive gliotransmitters like glutamate and ATP, and to mediate communication between glia and between glia and neurons (Perea & Araque, 2007; Agulhon *et al.* 2008; Fiacco *et al.* 2009). Gliotransmission has emerged in recent years as an additional layer of cellular communication that could contribute to information processing by the brain (Halassa & Haydon, 2010). However, the $Ca^{2+}$ signals required for gliotransmitter release, the release mechanism, and indeed the very existence of such release are highly controversial (Fiacco *et al.* 2009; Agulhon *et al.* 2010; Hamilton & Attwell, 2010).

One obstacle to a resolution of these questions is that astrocytes share many ligand-gated receptors with neurons (Fiacco *et al.* 2009). To activate astrocytes specifically, a transgenic mouse has been generated which selectively expresses a foreign G protein coupled receptor (GPCR) in astrocytes. Strikingly, in these mice, triggering specifically $Ca^{2+}$ elevations in astrocytes with a ligand had an effect neither on synaptic transmission and plasticity nor on neuronal excitability (Fiacco *et al.* 2007; Agulhon *et al.* 2010). This contrasts with other results showing $Ca^{2+}$-dependent gliotransmitter release (Perea & Araque, 2007; Andersson & Hanse, 2010; Gomez-Gonzalo *et al.* 2010; Halassa & Haydon, 2010). The reasons for these contradictory results are unclear (Agulhon *et al.* 2010; Halassa & Haydon, 2010).

The coupling between $Ca^{2+}$ signals and gliotransmitter release is still debated. Astrocytic $Ca^{2+}$ signals rely on plasma membrane receptors and channels, and on intracellular stores (Parpura *et al.* 2011) and near-membrane spontaneous and ATP-evoked $Ca^{2+}$ signals depend on different $Ca^{2+}$ sources (Shigetomi *et al.* 2010). This diversity of $Ca^{2+}$ signals could explain why different Gq GPCRs are not equally competent to triggering glutamate release (Shigetomi *et al.* 2008). A better understanding of $Ca^{2+}$-dependant gliotransmitter release will require the development of new specific tools for a reliable time-locked control of $Ca^{2+}$ signals, which need to be associated with imaging techniques for the simultaneous monitoring of $Ca^{2+}$ signals in electrically silent astrocytes. In an attempt to develop such methods, we set out to control astrocytic $Ca^{2+}$ rises using the light-gated $Ca^{2+}$-permeable ionotropic glutamate receptor 6 (LiGluR), the monovalent cationic channel channelrhodopsin 2 (ChR2), and the new $Ca^{2+}$-translocating channelrhodopsin (CatCh). These channels have been used for a remote non-invasive activation of neurons with high spatio-temporal resolution (Szobota *et al.* 2007; Gradinaru *et al.* 2009; Wyart *et al.* 2009), and ChR2 has been used to activate astrocyte-dependent neuronal responses *in vivo* (Gradinaru *et al.* 2009; Gourine *et al.* 2010).

Using cultured cortical astrocytes, we first show that LiGluR and, to a lesser extent, CatCh, provide a more reliable means for triggering reproducible intracellular $Ca^{2+}$ elevations than the enhanced ChR2 mutant (ChR2(H134R)). We then combined LiGluR activation with evanescent-field excitation $Ca^{2+}$ imaging to study the responses of LiGluR non-expressing (LiGluR(−)) astrocytes to the photoactivation of their LiGluR-expressing (LiGluR(+)) neighbours. We find that light-evoked $Ca^{2+}$ elevation in LiGluR(+) astrocytes triggers delayed short-lasting small-amplitude $Ca^{2+}$ transients in adjacent LiGluR(−) astrocytes, and that this LiGluR-evoked astrocyte-to-astrocyte communication involves a glutamate-permeable anion channel. Our results demonstrate the utility of LiGluR-based optogenetic approaches for studying communication between electrically silent cells.

## Methods

### Cell preparation, solutions and recording conditions

All experiments followed the European Union and institutional guidelines for the care and use of laboratory animals (Council directive 86/609EEC). Cortical astrocytes were prepared from P0–1 (P0 being the day of birth) NMRI mice as previously described (Li *et al.* 2009). The neocortex was dissected and mechanically dissociated. Cells were plated and maintained on poly-ornithine-coated coverslips (no. 1, BK-7, 25 mm diameter, Menzel-Gläser GmbH) for 1 week to reach confluence. Then, 0.15 mM dibutyryl cAMP (Sigma) was added to induce astrocyte differentiation into a more stellate morphology and form non-confluent islands of several astrocytes. All cultures were kept at 37°C in a humidified 5% $CO_2$ atmosphere. Primary astrocyte cultures were maintained in supplemented Dulbecco's modified Eagle's medium (DMEM, Invitrogen) with 5% fetal bovine serum (FBS), penicillin (5 U $ml^{-1}$) and streptomycin (5 $\mu g\ ml^{-1}$). The recordings were made during the following week.

For neuronal culture, cortical neurons and astrocytes were isolated from embryonic mice (E16). Cells were seeded on poly-L-lysine-treated coverslips and maintained in a medium containing minimum essential medium (MEM) with 5% FBS, 0.3% high glucose MEM, serum extender (1/1000) and penicillin/streptomycin (1/500). Cells were then maintained in half of this serum and half of medium of primary astrocytes containing growth factors for neurons. Cell media and supplements were from Invitrogen (Cergy Pontoise, France). Recordings were made at room temperature (RT) in solution containing

(in mM): 140 NaCl, 5.5 KCl, 1.8 $CaCl_2$, 1 $MgCl_2$, 20 glucose, 10 Hepes (pH 7.3, adjusted with NaOH). $Ca^{2+}$-free extracellular solutions contained nominally zero $Ca^{2+}$ and 5 mM EGTA.

## Fluorescent probes, reagents and plasmids

Cell media, supplements, $Ca^{2+}$ indicators (Fluo-4 AM, Xrhod-1 AM), and dyes (FM4–64, calcein AM, acridine orange, the mitochondrial marker pyridinium, 4-(2-(4-(dimethylamino)phenyl)ethenyl)-1-methyl iodide (DASPMI)) were purchased from Invitrogen (Cergy Pontoise, France), P2 receptor antagonists (pyridoxal-phosphate-6-azophenyl-2′,4′-disulfonate (PPADS), suramin, 2′-deoxy-$N^6$-methyladenosine 3′,5′-bisphosphate (MRS2179)), mGluR receptor antagonists ($\alpha$-methyl-4-carboxyphenylglycine (MCPG), 2-methyl-6-(phenylethynyl)pyridine (MPEP)), glutamate transporter inhibitor (DL-threo-$\beta$-benzyloxyaspartic acid (TBOA)) and thapsigargin were from Tocris (Bristol, UK), bafilomycin A1 from Calbiochem (Merck, Lyon, France) and all other compounds from Sigma-Aldrich. For fluorescence immunostaining experiments, we used the following antibodies: rabbit polyclonal glutamate antibody (1:200, ab9440, Abcam Inc., Cambridge, MA, USA) conjugated to the secondary antibody Alexa 594 goat anti-rabbit IgG (1:500, Invitrogen), mouse glial fibrillary acid protein (GFAP) monoclonal antibody (1:400, MAB360, Chemicon, Temecula, CA, USA) conjugated to the secondary antibody Alexa 488 goat anti mouse IgG (1:500, Invitrogen). Astrocytes were fixed with 1% paraformaldehyde and 0.1% glutaraldehyde (10 min, RT). After permeabilization and blockage of unspecific sites with phosphate buffered saline (PBS) 1×, 0.3% Triton X-100 and 2% bovine serum albumin (BSA) (1 h, RT), astrocytes were probed with respective primary antibody in the same solution overnight at 4°C. After being washed with PBS three times at RT, cells were incubated with secondary antibodies (2 h, RT). After three final washes (PBS, 10 min, RT), cells were mounted with Vectashield onto microscope slides. Immunostained cells were imaged with a Zeiss Axiovert LSM 510 confocal microscope using a ×63, NA 1.4 oil objective. Transfection was performed using lipofectamine 2000 (Invitrogen). Astrocytes were labelled with FM4–64 by incubating cells in dye-containing (6.7 $\mu$M) solution for 15 min and rinsing the cells for 30 min prior to imaging. $Ca^{2+}$ dyes were bulk-loaded into astrocytes as AM-esters in static dye-containing solutions (2 $\mu$M, 30 min for Fluo-4; 200 nM, 15 min for Xrhod-1). Another 30 min under continuous perfusion of dye-free solution allowed for the wash-off of extracellular dye and the complete de-esterification of the intracellular dye. During recording, cells were perfused at 0.5 ml $min^{-1}$ with standard extracellular solution. The glutamate-evoked $Ca^{2+}$ transients were induced by a brief (1 s) application of glutamate (100 $\mu$M) through a dual-channel local perfusion system, one continuously perfusing the control buffer and the other transiently delivering the glutamate-containing solution while the control channel was stopped. The solutions were delivered through plastic tubing (0.8 mm inner diameter, Tygon, Charny, France) to a multi-channel holder (AutoMate Scientific, Berkeley, CA, USA) connected to a small (250 $\mu$m ID) silica pipette (WPI, Saratosa, FL, USA).

## Fluorescence imaging

All combinations of excitation wavelengths and dichroic and emission filters used are listed in Supplemental Table 1. A custom-built inverted and upright microscope was used for bright-field, polychromatic epifluorescence imaging and through-the-objective (PlanApo TIRFM, ×60, 1.45 NA, Olympus, Hamburg, Germany) total internal reflection fluorescence microscopy (TIRFM). A Polychrome II (TILL Photonics, Gräfelfing, Germany) provided monochromatic (18 nm FWHM) epifluorescence (EPI) illumination. The 488 and 568 nm lines used for TIRFM were isolated from the beam of an Ar/Kr multi-line laser (CVI Melles Griot, Carlsbad, CA, USA) with an acousto-optical tuneable filter (AA.Opto, Saint Rémy de Chevreuse, France) and directed onto the glass–water interface at a super-critical angle. We estimated the effective penetration depth ($1/e^2$-intensity decay) of the order of 200 nm (Nadrigny *et al.* 2007). Fluorescence images were further magnified (×2) and projected on an electron multiplying charge-coupled device (EMCCD, QuantEM 512, Princeton Instruments, Trenton, NJ, USA). All devices were controlled by Metamorph (Molecular Devices, Downingtown, PA, USA). The effective pixel size in the sample plane was 133 nm. Time-lapse image stacks were taken at 0.5 Hz with 50–300 ms exposure times unless otherwise indicated.

Non-ratiometric $Ca^{2+}$ indicators (Fluo-4 and Xrhod-1) and TIRFM were used to monitor near-membrane $Ca^{2+}$ increases throughout this study, unless otherwise indicated. TIRFM confines illumination to the near-membrane, providing the conditions for sensitive detection of local $Ca^{2+}$ signals. Time-lapse fluorescence changes are plotted as $Ca^{2+}$-dependent fluorescence measured in 2 $\mu$m × 2 $\mu$m (15 pixel × 15 pixel) regions of interest (ROIs) normalized to the pre-stimulation baseline ($\Delta F/F_0$). The $Ca^{2+}$ elevations in LiGluR(−) cells were searched for by scanning such ROIs across the LiGluR(−) cell. To avoid a possible interference with light-evoked $Ca^{2+}$ rises in LiGluR(+) cells, $Ca^{2+}$ transients in LiGluR(−) cells were searched for in regions more than 2 $\mu$m away from the visible interface. Signalling events were identified as $\Delta F/F_0$ increases larger than

three times the standard deviation (SD) of the baseline. Traces were corrected for photobleaching as follows: individual reference traces were separately obtained by imaging dye-loaded cells without photoactivation, from which the mean decay time constant was obtained from a mono-exponential fit and then applied to correct the $Ca^{2+}$ traces in photostimulation experiments. $Ca^{2+}$ signals in astrocytes co-labelled with LiGluR–green fluorescent protein (GFP) and FM4–64 were imaged with Xrhod-1 following the triple-colour detection scheme as described previously (Li *et al.* 2008). Fluo-4 AM was used for $Ca^{2+}$ imaging of cells labelled with LiGluR–red fluorescent protein (RFP) and calcein. $Ca^{2+}$ imaging was performed ~5–10 min after pharmacological treatment of astrocytes unless otherwise stated. For the experiments done in zero $Ca^{2+}$, cells were kept in $Ca^{2+}$-free buffer for less than 5 min to avoid an interference with internal $Ca^{2+}$ stores (Li *et al.* 2008). Finally, $Ca^{2+}$ elevations were recorded only from cultured astrocytes showing no spontaneous $Ca^{2+}$ elevations.

### LiGluR, ChR2 and CatCh photoactivation

The engineering of LiGluR and synthesis of the tethered photoswitch maleimide-azobenzene-glutamate (MAG) have been previously described (Volgraf *et al.* 2006; Gorostiza *et al.* 2007; Numano *et al.* 2009). Cultured astrocytes were transfected with LiGluR-GFP, LiGluR-RFP, or cotransfected with LiGluR-RFP and AsRed under the control of the cytomegalovirus (CMV) promoter, using lipofectamine 2000 following the standard protocol. Cells were maintained in culture for 1–2 days after transfection to allow the proper targeting of LiGluR to the cell surface. Stock MAG solutions of 5–10 mM were prepared in anhydrous dimethyl sulfoxide (≥99.9%, Sigma) and stored at −20°C. To efficiently conjugate the photoswitch to LiGluR, MAG was pre-illuminated with 385 nm light (0.3 mW $mm^{-2}$) for 1 min (Gorostiza *et al.* 2007) before dilution in standard imaging solution to a final concentration of 10 $\mu$M. Transfected cells were then incubated in MAG-containing solution for 30 min in the dark followed by another 30 min washing with control buffer. During incubation, 5 $\mu$M concanavalin A (Sigma) was added to the medium to block LiGluR desensitisation (Numano *et al.* 2009). To switch on LiGluR, a 385 nm LED source (Thorlabs, Maisons Lafitte, France) was focused through an air objective (×10, NA 0.25, Olympus) to excite the cells in a 2 mm wide field, and the light pulse duration was 50–200 ms, unless otherwise stated. Where indicated, 488 nm light from the mono-chromator was used to EPI-illuminate the target cell and switch off LiGluR (39.1 mW $mm^{-2}$). Astrocytes and neurons were transfected with ChR2(H134R)-GFP using the same protocol as used for LiGluR, and examined 1–2 days after transfection. CatCh–yellow fluorescent protein (YFP) plasmid was provided by Dr Ernst Bamberg (MPI für Biophysik, Frankfurt, Germany). The red $Ca^{2+}$ dye Xrhod-1 (200 nm, 15 min) was used for $Ca^{2+}$ imaging of cells expressing ChR2 or CatCh. ChR2 and CatCh were photoactivated by 458 nm light (27.3 mW $mm^{-2}$ and 15.1 mW $mm^{-2}$, respectively) generated by the monochromator and delivered through the inverted epifluorescence pathway. For all light-gated channels, $Ca^{2+}$ imaging was temporally ceased during photoactivation and deactivation.

### Statistics

All data are expressed as mean ± standard deviation (SD), and Student's *t* test was used for testing the significance of *P* values. Non-normally distributed data were compared using their median ± absolute deviation and non-parametric tests (Kolmogorov–Smirnov, KS). All statistical operations used Matlab (The MathWorks, Natick, MA, USA). $^{*}P < 0.05$, $^{**}P < 0.01$, $^{***}P < 0.001$.

## Results

### Photoactivation of LiGluR triggers astrocytic $Ca^{2+}$ rises

LiGluR is a light-gated channel consisting of a synthetic cysteine-reactive photoisomerizable agonist MAG covalently attached to a cysteine-substituted ionotropic glutamate receptor GluR6 (Volgraf *et al.* 2006; Numano *et al.* 2009). To examine the ability of LiGluR to control astrocytic $Ca^{2+}$ increase, mouse cortical astrocytes in culture were transfected with LiGluR-RFP to which MAG was covalently attached. Short pulses of 385 nm light (0.3 mW $mm^{-2}$, 50 ms) evoked robust and reliable $Ca^{2+}$ rises monitored with the green-fluorescent $Ca^{2+}$ indicator Fluo-4 ($\Delta F/F_0 = 29.9 \pm 4.0\%$, $n = 23$ trials from 7 cells; Fig. 1*A*). Light-evoked $Ca^{2+}$ responses were neither observed in the absence of LiGluR-RFP ($-0.1 \pm 1.5\%$, $n = 5$ cells), nor in cells expressing LiGluR without MAG ($0.3 \pm 2.0\%$, $n = 5$ cells), nor in cells lacking LiGluR and MAG ($\Delta F/F_0 = 0.1 \pm 1.6\%$, $n = 5$ cells) (Supplemental Fig. 1*A*). The LiGluR-evoked $Ca^{2+}$ rises recorded in the thin processes of LiGluR(+) astrocytes were synchronized and their amplitude was maintained along the process as expected for a direct activation of LiGluR targeted to the process membrane (Fig. 1*B*). Finally, the amplitude of LiGluR-elicited $Ca^{2+}$ signals correlated with the duration of illumination (Supplemental Fig. 1*B*).

Besides being activated by UV light, LiGluR can be switched off with 488 nm blue light (Szobota *et al.* 2007). Because the spectral band for deactivating LiGluR overlaps with the 488 nm excitation

wavelength of Fluo-4, epifluorescence $Ca^{2+}$ imaging quickly terminates LiGluR-evoked responses (Supplemental Fig. 1*C* and *D*). To minimize imaging-light induced LiGluR deactivation, and to shape the $Ca^{2+}$ increases with a pulse of EPI-illumination deactivation, we confined $Ca^{2+}$ imaging to the near-membrane cellular compartment, using total internal reflection fluorescence microscopy (TIRFM) (Supplemental Fig. 1*E*). In these conditions, alternating pulses of 385 nm and 488 nm light evoked reproducible $Ca^{2+}$ transients (Fig. 1*C*). To minimize LiGluR deactivation during $Ca^{2+}$ imaging, we also used a LiGluR-GFP construct with the red-fluorescent $Ca^{2+}$ indicator Xrhod-1 AM. This combination allowed us to monitor LiGluR-evoked $Ca^{2+}$ responses ($\Delta F/F_0 = 31.3 \pm 6.0\%$, $n = 12$ trials from 5 cells), and to shape the $Ca^{2+}$ rise by altering the interval between the activating and deactivating light pulses (Fig. 1*D–F*). Together, these results indicate that photoactivation of LiGluR provides a robust, graded and reliable control of $Ca^{2+}$ signalling in astrocytes.

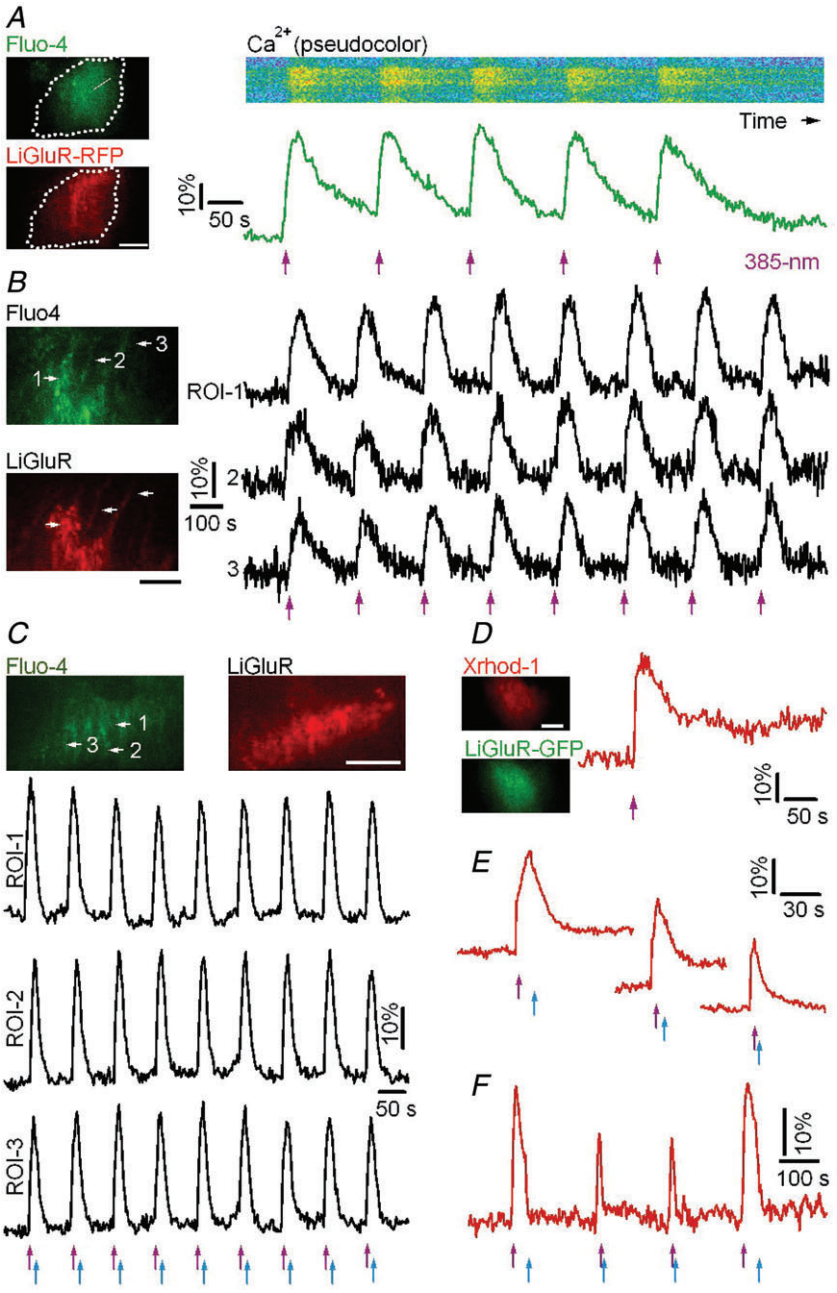


**Figure 1. LiGluR evokes precisely timed and shaped $Ca^{2+}$ rises in astrocytes**
*A*, dual-colour TIRF image of a cultured cortical astrocyte transfected with LiGluR-RFP conjugated with the photoswitch MAG and loaded with the green-fluorescent $Ca^{2+}$ indicator Fluo-4 (left). Dashed line shows the contour of the cell. The pseudocolour kymograph and green trace illustrate reproducible $Ca^{2+}$ rises evoked by 385 nm light pulses (violet arrows, 0.3 mW $mm^{-2}$, 50 ms). *B*, LiGluR photoactivation evoked repetitive and synchronized $Ca^{2+}$ rises in astrocytic soma (ROI-1) and processes (ROI-2 and ROI-3). *C*, temporal shaping of astrocytic $Ca^{2+}$ rises by switching LiGluR on and off with alternate 385 nm (violet arrows) and 488 nm (blue arrows, 39.1 mW $mm^{-2}$, 200 ms) EPI light pulses. *D–F*, astrocytic $Ca^{2+}$ elevations induced by LiGluR-GFP photoactivation and monitored with the red-fluorescent $Ca^{2+}$ indicator Xrhod-1. The $Ca^{2+}$ signals were shaped by switching off LiGluR with variable delay using 488 nm EPI light from the monochromator. Bars, 10 $\mu$m.

### Opsin-derived proteins are less efficient than LiGluR in triggering astrocytic $Ca^{2+}$ rises

Previous reports indicate that ChR2 can activate astrocytes (Gradinaru *et al.* 2009; Gourine *et al.* 2010); therefore we decided to compare the ability of ChR2 and LiGluR to elicit $Ca^{2+}$ elevations in astrocytes.

We first confirmed our ability to activate ChR2-expressing neurons in culture by showing that the repetitive photoactivation of ChR2(H134R) (Nagel *et al.* 2005) with 458 nm light pulses (27.3 mW $mm^{-2}$, 500 ms) evoked $Ca^{2+}$ transients (Fig. 2*A*) in 9 of 14 cortical neurons expressing ChR2(H134R)-GFP. Light-evoked $Ca^{2+}$ transients were absent in control neurons without

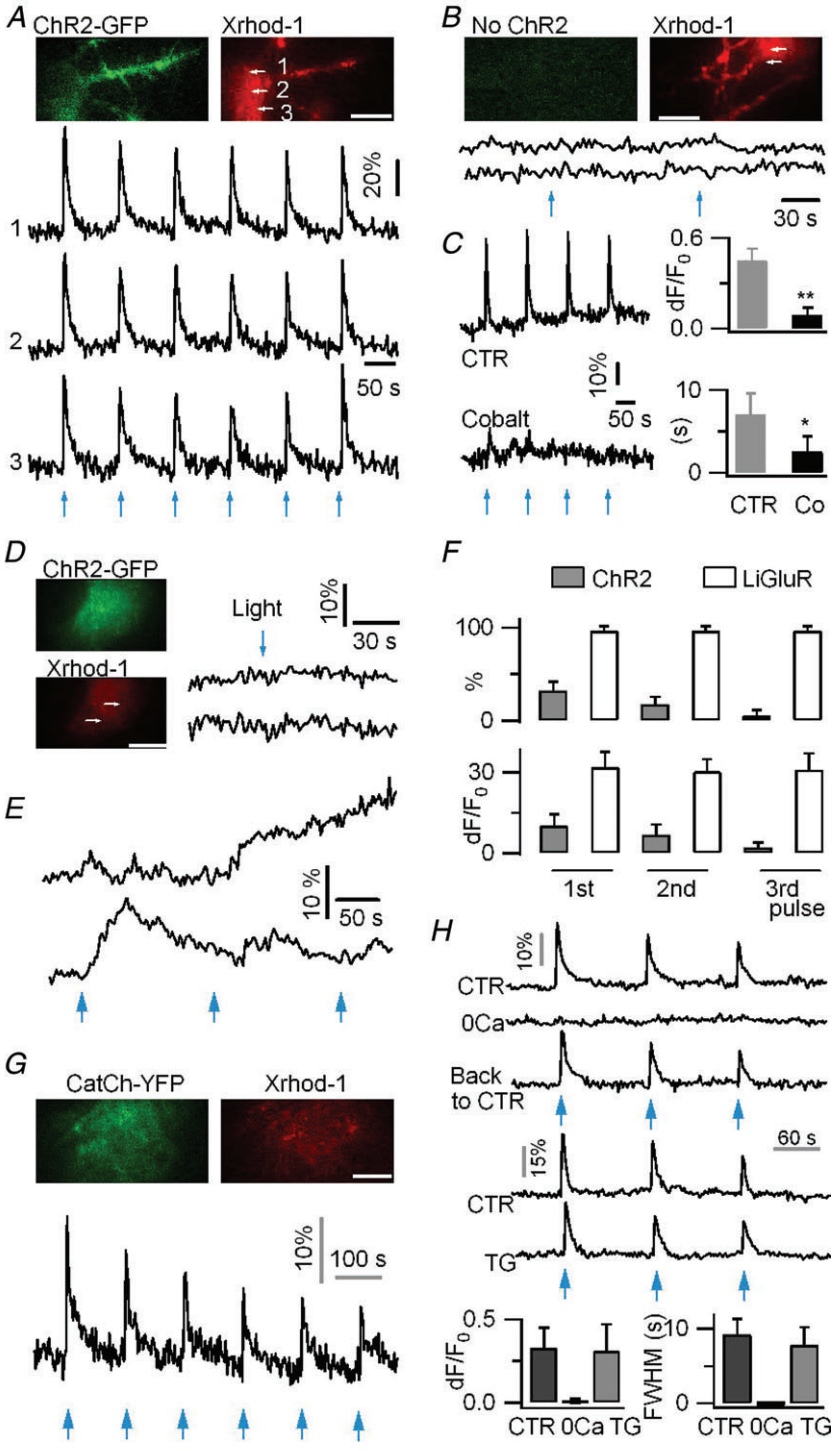


**Figure 2. $Ca^{2+}$ signalling in astrocytes evoked by photoactivation of the mutant channelrhodopsin ChR2(H134R) and the $Ca^{2+}$-permeable channelrhodopsin CatCh**
*A*, in a neuron expressing ChR2(H134R)-GFP and loaded with the red $Ca^{2+}$ indicator Xrhod-1, 458 nm EPI pulses (27.3 mW $mm^{-2}$, 500 ms) evoked reproducible $Ca^{2+}$ rises ($\Delta F/F_0 = 46.0 \pm 13.2\%$, $n = 9$ cells). *B*, absence of light-evoked $Ca^{2+}$ increases in neurons not expressing ChR2 ($\Delta F/F_0 = 1.3 \pm 6\%$, $n = 4$ cells). *C*, neuronal ChR2-evoked $Ca^{2+}$ rises were inhibited by the non-selective voltage-gated $Ca^{2+}$ channel (VGCC) blocker, cobalt (Co, 1 mM, $\Delta F/F_0 = 9.2 \pm 4.7\%$, FWHM $= 2.5 \pm 1.9$ s; *vs.* control $\Delta F/F_0 = 45.4 \pm 8.3\%$, $P < 0.01$, FWHM $= 7.0 \pm 2.6$ s, $P < 0.05$, $n = 8$ trials from 4 cells per condition). *D*, in astrocytes, short photoactivation (458 nm, 27.3 mW $mm^{-2}$, 500 ms) of ChR2 did not evoke any near-membrane $Ca^{2+}$ elevation. *E*, example $Ca^{2+}$ responses evoked by longer light pulse (458 nm, 1 s) in ChR2-expressing astrocytes. *F*, percentage of astrocytes showing light-gated $Ca^{2+}$ rises, and $Ca^{2+}$ response amplitude in LiGluR-expressing (60/63 cells) and ChR2-expressing (19/60 cells) astrocytes. The comparison was made using three successive light pulses (385 nm, 100 ms for LiGluR; 458 nm, 1 s for ChR2) applied every 150 s. *G*, in astrocytes, the photoactivation (1 s, 458 nm) of CatCh evokes fast $Ca^{2+}$ rises which fade upon repetitive photoactivation. *H*, CatCh-evoked $Ca^{2+}$ elevations in astrocytes were absent in 0 mM $Ca^{2+}$ extracellular solution (0 Ca, solution change was achieved in less than 30 s), and were unaffected by depleting the endoplasmic reticulum $Ca^{2+}$ store by thapsigargin (TG, 2 $\mu$M, 20 min). Recordings were done on the same cells in different conditions. CatCh photoactivation, 2 s 458 nm (CTR, 15 trials, 5 cells; 0 Ca, 6 trials, 3 cells; TG, 18 trials, 6 cells). Bars, 10 $\mu$m.

ChR2(H134R)-GFP (Fig. 2*B*), and were inhibited by cobalt, a non-selective blocker of voltage-gated $Ca^{2+}$ channels (VGCCs) (Fig. 2*C*), indicating that neuronal $Ca^{2+}$ rise is mainly due to a secondary entry via VGCCs.

We then expressed ChR2(H134R)-GFP in astrocytes. The average ChR2(H134R)-GFP fluorescence intensity was found to be comparable in astrocytes and neurons, suggesting that in our conditions, similar expression levels are achieved in both cell types (Supplemental Fig. 2*A*). The same light intensity used for neurons, however, evoked small $Ca^{2+}$ changes in cultured cortical astrocytes expressing ChR2(H134R) ($\Delta F/F_0 = 5.1 \pm 4.2\%$, $n = 5$, Fig. 2*D*), which were not significantly different from the control responses of ChR2-non-expressing cells ($\Delta F/F_0 = 2.2 \pm 3.0\%$, $n = 5$, $P = 0.3$). Longer (1 s) 458 nm light pulse occasionally evoked $Ca^{2+}$ increases in a subset of astrocytes, but responses were variable in duration and amplitude, as imaged with TIRFM (Fig. 2*E*) and epifluorescence (Supplemental Fig. 2*B*). In comparison with LiGluR, ChR2(H134R) was significantly less effective in driving astrocytic $Ca^{2+}$ elevation, in terms of light intensity and duration needed, percentage of responsive cells, and amplitude of light-evoked $Ca^{2+}$ responses (Fig. 2*F*). Our inability to trigger reliable $Ca^{2+}$ rises in astrocyte following ChR2(H134R) photoactivation could be due to a malfunction of this channel when expressed in astrocytes. To investigate this possibility, we compared the performance of ChR2(H134R) in astrocytes and neurons. Since ChR2 is highly permeable to $H^+$ (Nagel *et al.* 2003), the $H^+$ influx induced by its photoactivation is expected to quench the fluorescence of ChR2(H134R)-GFP (Nadrigny *et al.* 2006). We observed that ChR2(H134R) photoactivation induced a similar degree of quenching of intracellular ChR2(H134R)-GFP fluorescence in astrocytes and neurons (Supplemental Fig. 2*C*). This result indicates that ChR2(H134R) is as well-expressed and functional in astrocytes as it is in neurons. Thus, the relative inefficacy of ChR2 to trigger $Ca^{2+}$ rise in astrocytes might be due to its low $Ca^{2+}$ permeability. We therefore tested a recently developed $Ca^{2+}$-permeable channelrhodopsin mutant called CatCh (Kleinlogel *et al.* 2011). $Ca^{2+}$ rises could be triggered in astrocytes by optical activation of CatCh, although this required ~50 times more power and ~10 times longer illumination (15.1 mW mm$^{-2}$, 1 s) than with LiGluR and, unlike the reproducible LiGluR-evoked responses, the CatCh-evoked responses faded in amplitude with repeated stimulation (Fig. 2*G*). Our results indicate that $Ca^{2+}$-permeable LiGluR and, to a lesser extent, CatCh are more efficient than ChR2 in controlling astrocytic $Ca^{2+}$ elevation.

We next examined the cellular mechanisms of the $Ca^{2+}$ increase evoked in astrocytes by the photoactivation of CatCh and LiGluR. CatCh is a light-sensitive $Ca^{2+}$-permeable ChR2 (Kleinlogel *et al.* 2011), and CatCh-evoked $Ca^{2+}$ transients were abolished in 0 mM $Ca^{2+}$ (Fig. 2*H*). The endoplasmic reticulum (ER) $Ca^{2+}$ stores contribute to $Ca^{2+}$ signalling in astrocytes (Agulhon *et al.* 2008), but do not seem to be involved in CatCh-evoked $Ca^{2+}$ rises, since the application of thapsigargin (TG, 1 $\mu$M), which induced long-lasting cytoplasmic $Ca^{2+}$ rises reflecting the leak of $Ca^{2+}$ from ER stores ($\Delta F/F_0 = 71.7 \pm 10.4\%$, $n = 3$; Fig. 3*D*), had no effect on the subsequent CatCh-evoked $Ca^{2+}$ rises (Fig. 2*H*). These results suggest that CatCh-evoked $Ca^{2+}$ transients depend only on $Ca^{2+}$ influx.

LiGluR is derived from the kainate-type glutamate receptor GluR6 (Volgraf *et al.* 2006), and in line with previous reports (Gorostiza *et al.* 2007; Numano *et al.* 2009), the competitive AMPA/kainate receptor antagonist NBQX attenuated the LiGluR-evoked $Ca^{2+}$ increase ($\Delta F/F_0 = 19.3 \pm 9.7\%$, $n = 12$ trials from 4 cells, *vs.* control, $43.2 \pm 8.5\%$, $n = 15$ trials from 5 cells, $P < 0.01$; Fig. 3*A*). As predicted by the high $Ca^{2+}$ permeability of GluR6 (Egebjerg & Heinemann, 1993), the photoactivation of LiGluR in 0 mM $Ca^{2+}$ failed to trigger detectable $Ca^{2+}$ rises ($\Delta F/F_0 = 0.32 \pm 1.4\%$, $n = 5$), while the $Ca^{2+}$ rises evoked in 5 mM extracellular $Ca^{2+}$ ($\Delta F/F_0 = 45.2 \pm 14.3\%$, FWHM $= 97.1 \pm 43.8$ s, $n = 15$ trials from 5 cells) were larger than the control response evoked in 1.8 mM $Ca^{2+}$ ($\Delta F/F_0 = 21.6 \pm 6.7\%$, $P < 0.01$; FWHM $= 71.3 \pm 14.7$ s, $P < 0.05$; $n = 15$ trials from 5 cells; Fig. 3*B*). The $Ca^{2+}$ influx through the ion channel should lead to a rapid rise of the near-membrane $Ca^{2+}$ concentration detectable with TIRFM (Demuro & Parker, 2005). Sampling LiGluR-evoked $Ca^{2+}$ rises at 100 Hz, we captured an intermediate $\Delta F/F_0$ step one frame after light activation (Fig. 3*C*, red arrow), suggesting that the $Ca^{2+}$ rise occurs within 10 ms after LiGluR activation. We then tested a possible involvement of the $Ca^{2+}$ stores in LiGluR-evoked $Ca^{2+}$ signalling using thapsigargin (TG, 1 $\mu$M, 15 min) to block the ER $Ca^{2+}$-ATPase and deplete the $Ca^{2+}$ stores prior to LiGluR activation. Surprisingly, we found that LiGluR-evoked $Ca^{2+}$ rises were enhanced in TG-treated cells ($\Delta F/F_0 = 56.3 \pm 16.8\%$, $n = 17$ trials from seven cells, *vs.* control, $23.4 \pm 6.2\%$, $n = 19$ trials from 8 cells, $P < 0.01$; Fig. 3*E*). These results indicate that LiGluR-evoked $Ca^{2+}$ elevations rely on $Ca^{2+}$ influx, and that $Ca^{2+}$ uptake into the ER via the $Ca^{2+}$-ATPase limits the LiGluR-evoked cytosolic $Ca^{2+}$ increase.

## All optical probing of astrocyte-to-astrocyte communication with LiGluR

Having established LiGluR as a tool for controlling astrocytic $Ca^{2+}$ in culture, we investigated if LiGluR-evoked $Ca^{2+}$ increases can trigger gliotransmitter release. After transfection, only a subset of astrocytes express LiGluR, while the entire population of astrocytes

can be loaded with acetoxymethyl ester (AM) derivative of $Ca^{2+}$ indicators (Fig. 4*A*). This permitted us to explore astrocyte-to-astrocyte signalling in an all-optical manner, in which light was used to drive $Ca^{2+}$ elevation in LiGluR expressing (LiGluR(+)) cells as well as to report $Ca^{2+}$ signals in both the LiGluR(+) and adjacent LiGluR(−) astrocytes. To avoid interference with spontaneous $Ca^{2+}$ oscillations, recordings were made from astrocytes without spontaneous activity.

Photoactivation of LiGluR(+) was obtained using a UV 385 nm light-emitting diode (LED) and a ×10, NA 0.25 objective. All LiGluR(+) and LiGluR(−) astrocytes within a region of ∼2 mm diameter were exposed to UV light. Simultaneously, $Ca^{2+}$ signals in both LiGluR(+) cells and LiGluR(−) neighbouring cells were imaged using the ×60, NA 1.45 TIRF objective in a field of view of 50 × 50 $\mu$m, divided in two by a dual viewer. We found that the light-gated $Ca^{2+}$ rises in LiGluR(+) astrocytes triggered asynchronous $Ca^{2+}$ transients in adjacent LiGluR(−) astrocytes (Fig. 4*B*) in ∼35% of cell pairs (21/60). Tuning the amplitude and duration of the light-evoked $Ca^{2+}$ increases in the LiGluR(+) astrocytes over a wide range, we found that the threshold $Ca^{2+}$ integral in the LiGluR(+) astrocyte needed to trigger $Ca^{2+}$

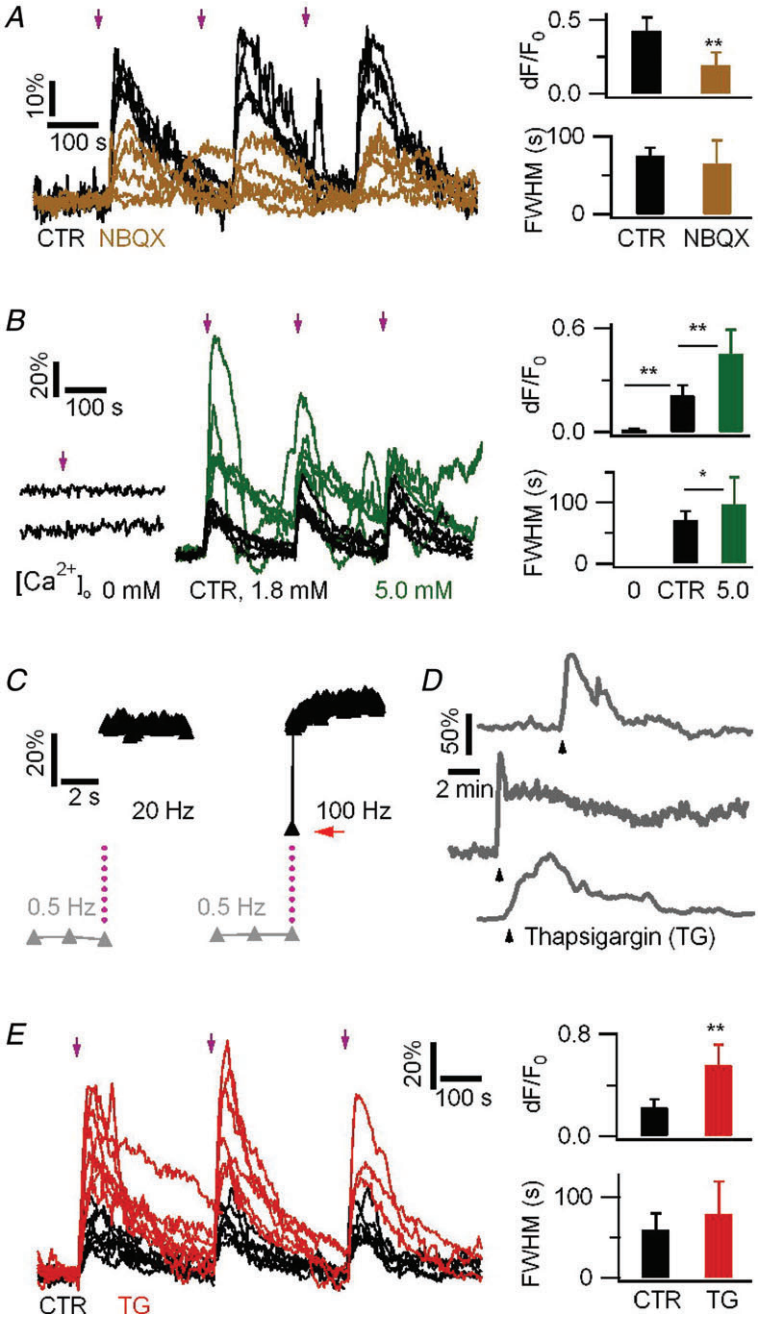


**Figure 3. LiGluR-evoked near-membrane $Ca^{2+}$ rises in astrocytes depend on $Ca^{2+}$ influx and uptake into the endoplasmic reticulum**
*A*, LiGluR-evoked $Ca^{2+}$ responses in the absence (control, 12 trials from 4 cells) and in the presence (15 trials, 5 cells) of a competitive GluR6 antagonist NBQX (1 mM). LiGluR-RFP and the green $Ca^{2+}$ indicator Fluo-4 were used. *B*, LiGluR-evoked $Ca^{2+}$ responses in zero $Ca^{2+}$ (5 trials, 5 cells, left), 1.8 mM $Ca^{2+}$ (control, 15 trials from 5 cells, middle, black traces), and 5 mM $Ca^{2+}$ (15 trials, 5 cells; green traces). *C*, LiGluR activation triggers a rapid near-membrane $Ca^{2+}$ increase (grey triangles, 0.5 Hz imaging prior to photoactivation. Black triangles, 20 and 100 Hz imaging after 10 ms activation light pulse, purple dots). An intermediate rising step, indicated by a red arrow, was revealed at 100 Hz. Similar results were obtained for six astrocytes. *D*, the $Ca^{2+}$-ATPase inhibitor thapsigargin (TG, 1 $\mu$M) led to $Ca^{2+}$ elevation due to $Ca^{2+}$ release from the internal store. Black arrowhead indicates the beginning of TG application, which was maintained throughout the recording. Each trace depicts the response of a single astrocyte. *E*, inhibition of $Ca^{2+}$-ATPase by TG (1 $\mu$M, 15 min) enhanced LiGluR-evoked $Ca^{2+}$ increases (red, 17 trials, 7 cells, *vs.* control, black, 19 trials, 8 cells. n.s. $P > 0.16$).

transients in LiGluR(−) neighbours was larger than a reference $Ca^{2+}$ signal (Ref-Ca) evoked by a 1 s application of 100 $\mu$M glutamate (Fig. 4*C* and *E*), a concentration that is in the physiological range of the glutamate encountered by astrocytes *in situ* (Dzubay & Jahr, 1999). A LiGluR-evoked $Ca^{2+}$ signal mimicking Ref-Ca did not trigger statistically significant $Ca^{2+}$ transients in adjacent LiGluR(−) cells ($\Delta F/F_0 = 3.8 \pm 3.9\%$, $n = 15$, *vs.* control in non-transfected cell pairs, $0.9 \pm 2.3\%$, $n = 5$, $P = 0.15$; Fig. 4*D*).

Unlike the direct LiGluR-evoked $Ca^{2+}$ signals in the processes of LiGluR(+) astrocytes which were time-locked with the light pulses, the $Ca^{2+}$ transients detected in adjacent LiGluR(−) astrocytes were local, asynchronous (Fig. 4*B*), smaller in peak amplitude, shorter lasting (Fig. 4*F*), and occurred after a variable delay

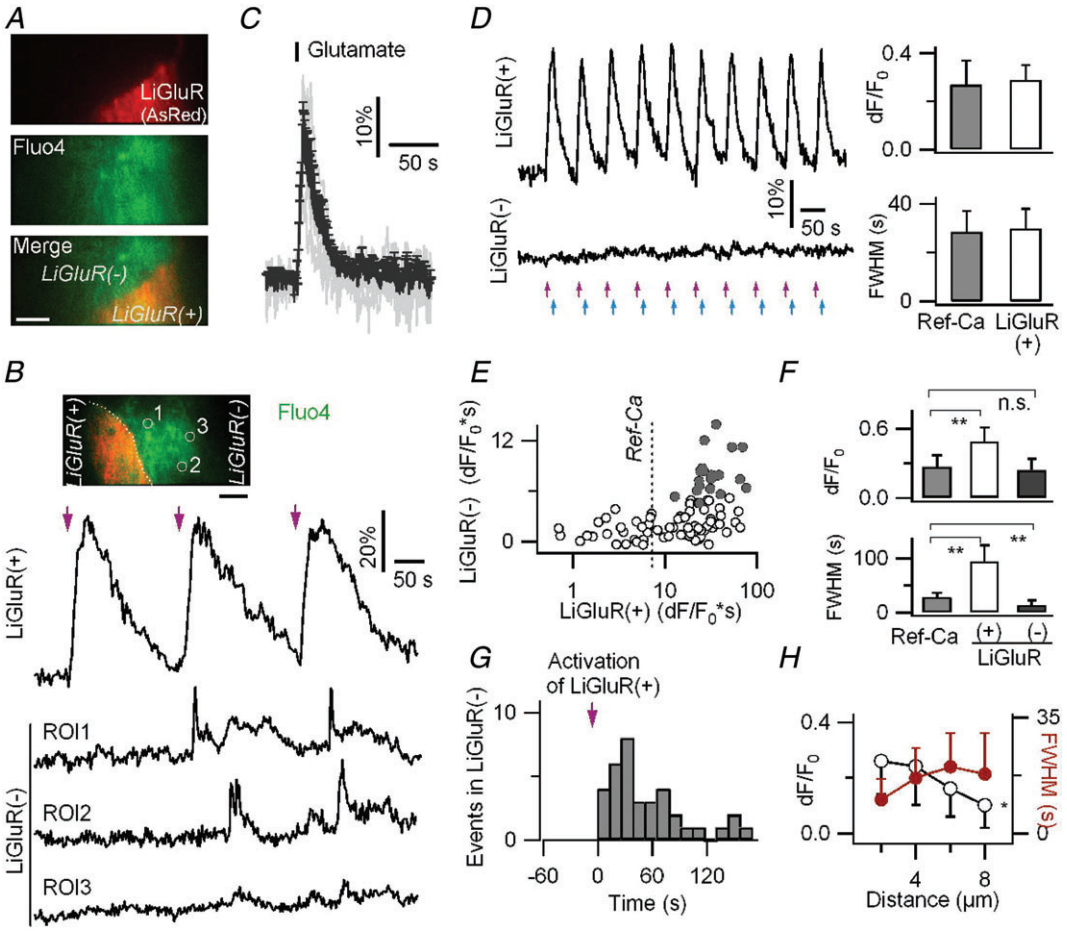


**Figure 4. All optical probing of astrocyte-to-astrocyte communication using LiGluR and TIRF**
*A*, AsRed was co-transfected with LiGluR-RFP to identify the border between LiGluR-RFP/AsRed-expressing (LiGluR(+)) and LiGluR-RFP/AsRed-non-expressing (LiGluR(−)) astrocytes. Fluo-4 AM was used to monitor $Ca^{2+}$ activity in LiGluR(+) and LiGluR(−) astrocytes. *B*, light-evoked near-membrane $Ca^{2+}$ rises in a LiGluR(+) astrocyte induced asynchronous short-lasting small-amplitude $Ca^{2+}$ rises in an adjacent LiGluR(−) astrocyte. Light pulses are indicated by violet arrows. *C*, astrocytic $Ca^{2+}$ elevations (individual traces in grey; average ± SD in black) evoked by glutamate application (100 $\mu$M, 1 s, 8 cells). The average response was designated as the reference $Ca^{2+}$ response (Ref-Ca). *D*, repetitive light activation tuned to evoke $Ca^{2+}$ rises in a LiGluR(+) astrocyte with peak amplitude ($\Delta F/F_0$) and half-duration (FWHM) matching the Ref-Ca (right, $P > 0.7$) did not trigger measurable near membrane $Ca^{2+}$ responses in the neighbouring LiGluR(−) astrocyte. *E*, relative distribution of the integral over time ($\Delta F/F_0^*$s) of the light-evoked $Ca^{2+}$ increases in LiGluR(+) astrocytes and LiGluR(−) astrocytes (85 cell pairs). Filled circles represent pairs in which $Ca^{2+}$ transients were detected in LiGluR(−) cells ($n = 20$). The dotted line indicates the integral of the Ref-Ca signal. *F*, in comparison with the Ref-Ca signal, the LiGluR-evoked $Ca^{2+}$ rises in LiGluR(+) astrocytes was larger and longer lasting, while the $Ca^{2+}$ transients detected in LiGluR(−) astrocytes showed a similar amplitude but a shorter duration (19 events, 5 cells; n.s., $P = 0.8$). *G*, temporal distribution of the LiGluR-evoked $Ca^{2+}$ transients detected in LiGluR(−) astrocytes relative to the initiation of photoactivated $Ca^{2+}$ rises in LiGluR(+) astrocytes (32 events, 14 cells, bi$n = 8$ s). *H*, peak amplitude ($\Delta F/F_0$) and half-duration (FWHM) of the LiGluR-evoked $Ca^{2+}$ transients in LiGluR(−) astrocytes as a function of the distance from the visible interface between LiGluR(+) and LiGluR(−) astrocytes ($n = 4$–12 per condition). Bars, 5 $\mu$m.

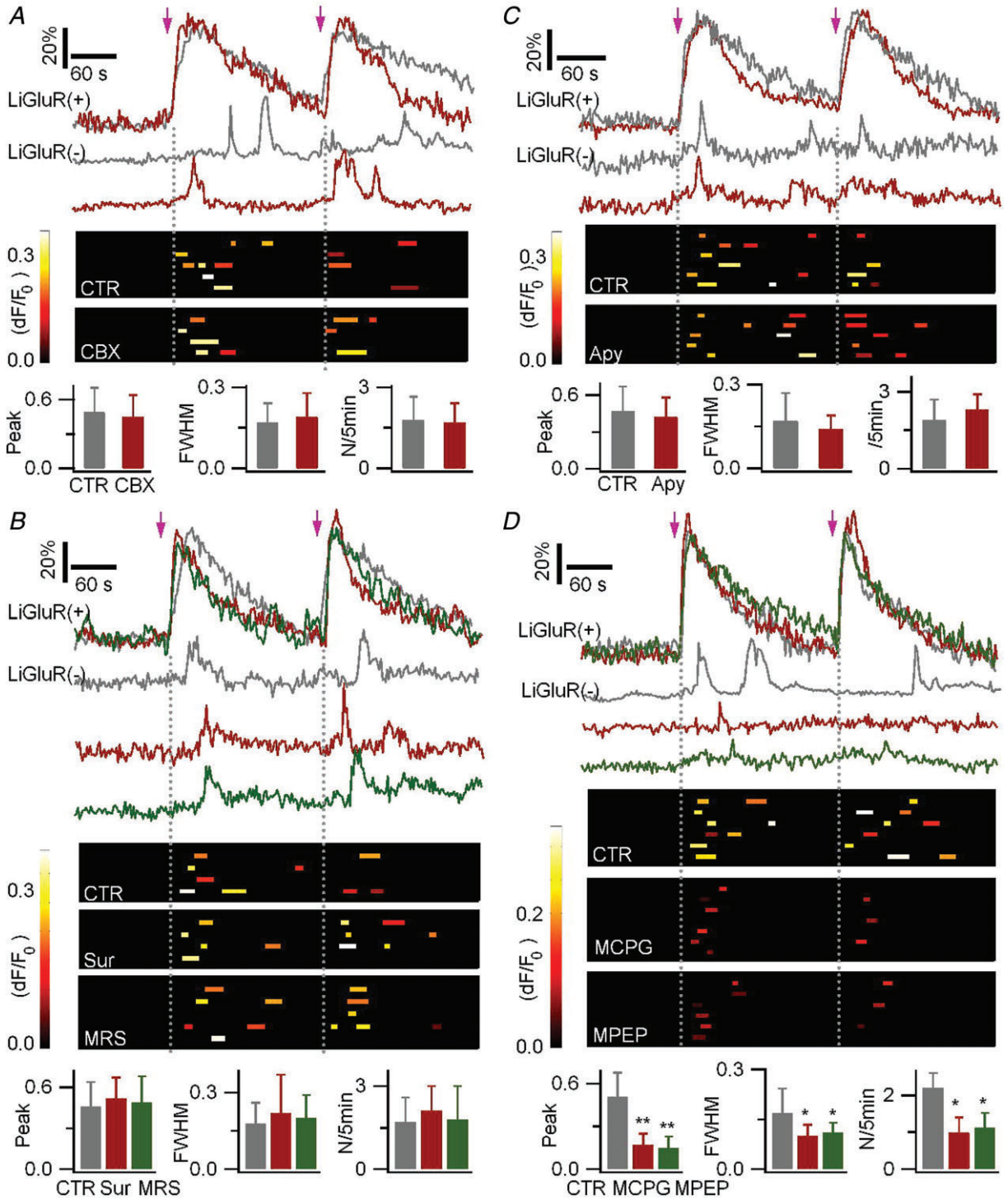


**Figure 5. LiGluR-evoked astrocyte-to-astrocyte communication is mediated by glutamate release**
To monitor $Ca^{2+}$ activity in LiGluR(+) and LiGluR(−) cells, astrocytes were co-transfected with LiGluR-RFP and AsRed, and loaded with Fluo-4 AM. *A*, the gap junction blocker carbenoxolone (CBX) had no effect on the LiGluR-evoked $Ca^{2+}$ rises in LiGluR(−) astrocytes. Light pulses are indicated by arrows. Top, $\Delta F/F_0$ sample traces in a LiGluR(+) cells and an adjacent LiGluR(−) cells in control (CTR, grey traces) and in carbenoxolone (CBX, 100 $\mu$M, red traces). Middle, summary plots of the near-membrane $Ca^{2+}$ rises detected in LiGluR(−) cells. Each row represents a single cell, each bar represents a single event (larger than 3SD of the background noise), its location on the *x*-axis reflects its timing, bar length reflects its half-duration (FWHM), and its peak amplitude ($\Delta F/F_0$) is encoded in pseudocolour. Bottom, summary data of the relative peak amplitude and FWHM, both normalized to the corresponding $Ca^{2+}$ rises in LiGluR(+) cells, and the occurrence frequency (N/5 min) of the

(36.0 ± 26.2 s, median ± absolute deviation, $n = 37$ events in 15 cells; Fig. 4*G*). The amplitude and width of the $Ca^{2+}$ responses in LiGluR(−) astrocytes also varied with the distance from the boundary between two cells (Fig. 4*H*). Such localized astrocytic $Ca^{2+}$ signals resemble those seen *in situ* (Wang *et al.* 2006; Gordon *et al.* 2009; Agulhon *et al.* 2010), suggesting that LiGluR-evoked $Ca^{2+}$ rises in cultured astrocytes mediate a chemical communication to adjacent LiGluR(−) astrocytes.

## LiGluR-evoked astrocyte-to-astrocyte communication is due to glutamate release

Having observed what appears to be a LiGluR-evoked signalling between adjacent astrocytes, we sought to identify the cellular mechanism underlying this astrocyte-to-astrocyte communication.

Second messengers such as $IP_3$ or $Ca^{2+}$ are suggested to diffuse between astrocytes through gap junctions (Scemes & Giaume, 2006). The gap junction blocker carbonoxolone had no effect on the light-evoked $Ca^{2+}$ rises in LiGluR(+) astrocytes (Supplemental Table 2), and did not interfere with the $Ca^{2+}$ transients in adjacent LiGluR(−) cells (Fig. 5*A*), suggesting that the LiGluR-evoked astrocyte-to-astrocyte signal is not due to gap junction communication but to the release of a transmitter into the external medium.

ATP, a gliotransmitter candidate, induces type-2 purinergic receptor (P2R)-mediated $Ca^{2+}$ rises in astrocytes (Fam *et al.* 2000). To test the possibility of LiGluR-evoked ATP release, we studied the effect of P2R antagonists on the LiGluR-evoked $Ca^{2+}$ transients in LiGluR(−) astrocytes. As the P2R antagonist PPADS interfered with the LiGluR-evoked $Ca^{2+}$ rises in LiGluR(+) astrocytes (Supplemental Table 2), we tested another P2R antagonist, suramin (100 $\mu$M), and a P2Y1 receptor antagonist, MRS2179 (25 $\mu$M), which both reduced the ATP-evoked $Ca^{2+}$ rises (Supplemental Fig. 3*A*), without having an effect on LiGluR-evoked $Ca^{2+}$ signals in LiGluR(+) astrocytes (Supplemental Table 2). Both antagonists had no effect on the LiGluR-evoked $Ca^{2+}$ transients in LiGluR(−) astrocytes (Fig. 5*B*). We also tested the effect of the ectonucleotidase apyrase, which degrades extracellular ATP and inhibits purinergic signalling in astrocytes (Stout *et al.* 2002; Bowser & Khakh, 2007). Control experiments showed that apyrase had no effect on the LiGluR-evoked $Ca^{2+}$ rise in LiGluR(+) cells (Supplemental Table 2). We found that apyrase did not alter the $Ca^{2+}$ transients in LiGluR(−) astrocytes (Fig. 5*C*). Together, these results indicate that LiGluR-evoked astrocyte-to-astrocyte communication is not due to ATP release.

Glutamate, another gliotransmitter candidate, activates metabotropic glutamate receptors (mGluR) and mediates $Ca^{2+}$ rise in astrocytes (Gordon *et al.* 2009; Sasaki *et al.* 2011). The group I mGluR5 mediates astrocytic $Ca^{2+}$ elevation via the phospholipase C (PLC) $IP_3$ pathway (Cai *et al.* 2000; Fiacco *et al.* 2009). To test the possibility of LiGluR-evoked glutamate release, we used a wide-spectrum antagonist, MCPG, to block the group I/II mGluRs, and MPEP, a mGluR5 antagonist. Neither MCPG nor MPEP had an effect on LiGluR-evoked $Ca^{2+}$ signals in LiGluR(+) astrocytes (Supplemental Table 2). Both, applied separately, reduced LiGluR-evoked transient $Ca^{2+}$ rises in LiGluR(−) astrocytes (Fig. 5*D*). Altogether, these results suggest that LiGluR-evoked $Ca^{2+}$ transients in LiGluR(−) astrocytes are mediated by glutamate release from LiGluR(+) astrocytes, and they establish LiGluR as a potent tool to study the mechanisms of intercellular communication between electrically silent cells such as the protoplasmic astrocytes.

## Exocytosis is not a major route for LiGluR-evoked glutamate release by astrocyte

We next decided to investigate possible pathways of LiGluR-evoked glutamate release, such as reverse transport (Rossi *et al.* 2000), vesicular release (Hamilton & Attwell, 2010), hemichannels (Ye *et al.* 2003), and anion channels (Takano *et al.* 2005; Kimelberg *et al.* 2006; Park *et al.* 2009).

The possible involvement of a glutamate transporter (Rossi *et al.* 2000) is unlikely since we found no effect of the transporter blocker TBOA on LiGluR-evoked $Ca^{2+}$ transients in LiGluR(−) astrocytes (Supplemental Fig. 3*B*; Supplemental Table 2).

$Ca^{2+}$ rises in LiGluR(−) astrocytes in CTR (12 events, 5 cells) and CBX (9 events, 4 cells; $P > 0.6$). *B*, top, sample traces in control (grey traces), in the presence of the P2 purinergic receptor antagonist suramin (Sur, 100 $\mu$M, red traces), and P2Y1 receptor antagonist MRS2179 (MRS, 25 $\mu$M, green traces). Middle, summary plots of the $Ca^{2+}$ events in LiGluR(−) cells as defined in *A*. Bottom, summary data in control ($n = 9$ events, 4 cells), suramin (11 events, 4 cells), and MRS2179 (12 events, 5 cells; $P > 0.23$). *C*, apyrase (20 U ml$^{-1}$) did not inhibit the LiGluR-evoked $Ca^{2+}$ transients in the LiGluR(−) cells. Sample traces, and summary plots of the evoked $Ca^{2+}$ transients in control (15 events, 6 cells), and in apyrase (Apy, $n = 16$ events, 5 cells; $P > 0.26$). *D*, LiGluR-evoked $Ca^{2+}$ transients in the LiGluR(−) cells in control ($n = 18$ events, 6 cells; grey traces) were reduced in amplitude, duration, and frequency by the group I/II mGluR antagonist MCPG (500 $\mu$M, 9 events, 6 cells; red traces) and the mGluR5 antagonist MPEP (100 $\mu$M, 9 events, 7 cells; green traces).

We next investigated the possibility of $Ca^{2+}$-regulated exocytosis (Hamilton & Attwell, 2010). We previously showed that astrocytic lysosomes undergo asynchronous $Ca^{2+}$-regulated exocytosis (Li *et al.* 2008), and recent findings suggest that the lysosomal $H^+$/sialic acid cotransporter, sialin, is a vesicular aspartate/glutamate transporter (Miyaji *et al.* 2008), raising the possibility of LiGluR-evoked glutamate release by lysosomal exocytosis. To test this possibility, we used the styryl dye FM4–64 to monitor lysosomal exocytosis (Zhang *et al.* 2007; Li *et al.* 2008) in LiGluR-transfected astrocytes. Control experiments showed that LiGluR photoactivation evoked similar $Ca^{2+}$ rises in LiGluR(+) astrocytes in control and after FM4–64 loading ($\Delta F/F_0 = 47.6 \pm 5.1\%$, FWHM $= 65.3 \pm 6.1$ s, *vs.* control, $\Delta F/F_0 = 49.4 \pm 6.8\%$, FWHM $= 50.3 \pm 9.5$ s, $n = 6$ trials from 3 cells, $P > 0.14$; Fig. 6*Aa*). We found that the LiGluR-evoked $Ca^{2+}$ had no effect on the fluorescence of FM4–64-labelled lysosomes ($\Delta F/F_0$, $-1.1 \pm 4.5\%$, $n = 23$ lysosomes from 5 LiGluR(+) cells, *vs.* control, $0.9 \pm 2.6\%$, $n = 12$ lysosomes from 3 LiGluR(−) cells, $P = 0.6$; Fig. 6*A*), indicating that lysosomal exocytosis is not a likely pathway for LiGluR-evoked glutamate release.

Astrocytes contain small synaptic-like vesicles which are suggested to carry glutamate vesicular transporters and undergo $Ca^{2+}$-dependent exocytosis (Bezzi *et al.* 2004; Hamilton & Attwell, 2010). Both lysosomes and small synaptic-like vesicles are acidic compartments. To test a possible involvement of all these acidic vesicles in the LiGluR-evoked glutamate release, we used the V–ATPase inhibitor bafilomycin A1 to disrupt the vesicular proton gradient (Bowman *et al.* 1988; Zhou *et al.* 2000; Angulo *et al.* 2004; Fiacco *et al.* 2007). Since long-term bafilomycin treatment can cause cell death (Nakashima *et al.* 2003), we made control experiments measuring mitochondrial fragmentation, a sign of cell death (Frank *et al.* 2001) (Supplemental Fig. 4*A*). We found that a limited (1 h) treatment, which affects minimally the mitochondria, is sufficient to abolish the vesicular pH gradient, as shown by the disruption of vesicular accumulation of the fluorescent weak base acridine orange (Fig. 6*B*). This bafilomycin treatment affected neither the LiGluR-evoked $Ca^{2+}$ rise in LiGluR(+) astrocytes (Supplemental Table 2), nor the LiGluR-evoked $Ca^{2+}$ transients in LiGluR(−) astrocytes (Fig. 6*C*), arguing against an involvement of acidic compartments in LiGluR-evoked glutamate release.

To further investigate a possible involvement of the synaptic-like small vesicles in LiGluR-evoked glutamate release, we used tetanus toxin (TeTx), an exocytosis blocker which cleaves VAMP2 (synaptobrevin II) and VAMP3 (cellubrevin) (McMahon *et al.* 1993) v-SNARE proteins suggested to be expressed by small astrocytic vesicles (Hamilton & Attwell 2010). Since bath application of TeTx did not cleave effectively the v-SNARE proteins as shown by the residual vesicular targeting of VAMP2–enhanced green fluorescent protein (EGFP) and VAMP3-EGFP (Supplemental Fig. 4*B*), we transfected astrocytes with the TeTx light chain to abolish the v-SNARE vesicular targeting (Fig. 6*D–E*). Astrocytes co-transfected with TeTx and LiGluR responded normally to light activation (Supplemental Table 2), and LiGluR-evoked $Ca^{2+}$ signals in LiGluR(−) astrocytes were unchanged (Fig. 6*F*), suggesting that VAMP2/3-dependant exocytosis is not involved in LiGluR-evoked glutamate release from astrocytes. Altogether these results indicate that the LiGluR-evoked glutamate release in astrocytes does not involve the exocytosis of either lysosomes or of small synaptic-like vesicles.

## LiGluR-evoked glutamate release from astrocyte via anion channels

Previous experiments suggest that glutamate release from astrocytes can also be mediated by non-selective hemichannels (Ye *et al.* 2003) and anion channels (Takano *et al.* 2005; Kimelberg *et al.* 2006; Park *et al.* 2009).

We first studied the effect of LiGluR activation on the fluorescence of calcein, a hemichannel-permeant dye (Stout *et al.* 2002; Thompson *et al.* 2006). Control experiments showed that mechanical stimulation without membrane rupture (Li *et al.* 2008) induced significant calcein release as expected from hemichannel opening (Stout *et al.* 2002) ($-26.3 \pm 7.9\%$ in 20 s, $n = 5$; Supplemental Fig. 5*A*), and that LiGluR-evoked $Ca^{2+}$ elevations in LiGluR(+) astrocytes were similar in control and in calcein-loaded astrocytes (Fig. 7*Aa*). We showed that the calcein fluorescence in LiGluR(+) astrocytes was unchanged by the LiGluR-evoked $Ca^{2+}$ elevation ($\Delta F/F_0 = -2.2 \pm 3.6\%$, *vs.* $-0.6 \pm 1.2\%$ in control cells without LiGluR, $n = 7$, $P = 0.33$; Fig. 7*A*). These results, together with the lack of effect of carbenoxolone (Fig. 5*A*), argue against the idea of LiGluR-evoked hemichannel-mediated glutamate release in astrocytes.

We next turned to anion channel blockers, flufenamic acid (FFA) and 5-nitro-2-(3-phenylpropylamino) benzoic acid (NPPB), which did not significantly affect LiGluR-evoked $Ca^{2+}$ rise in LiGluR(+) astrocytes (Supplemental Table 2). However, each blocker caused a reduction of the LiGluR-evoked $Ca^{2+}$ signalling in LiGluR(−) astrocytes ($\Delta F/F_0 = 0.25 \pm 0.1$ for FFA, $0.21 \pm 0.11$ for NPPB, *vs.* control, $0.52 \pm 0.14$, $n = 7$–12 events, $P < 0.01$; Fig. 7*B*). Hypotonic solutions induce cell swelling, anion channel opening, and enhance glutamate release, the hypertonic solutions having opposite effects (Takano *et al.* 2005; Kimelberg *et al.* 2006; Duran *et al.* 2010). As shown previously (Benfenati *et al.* 2011), hypotonic (−17%) solution induced $Ca^{2+}$ rises in astrocytes (Supplemental Fig. 5*B*), and therefore we could not perform competition experiments and

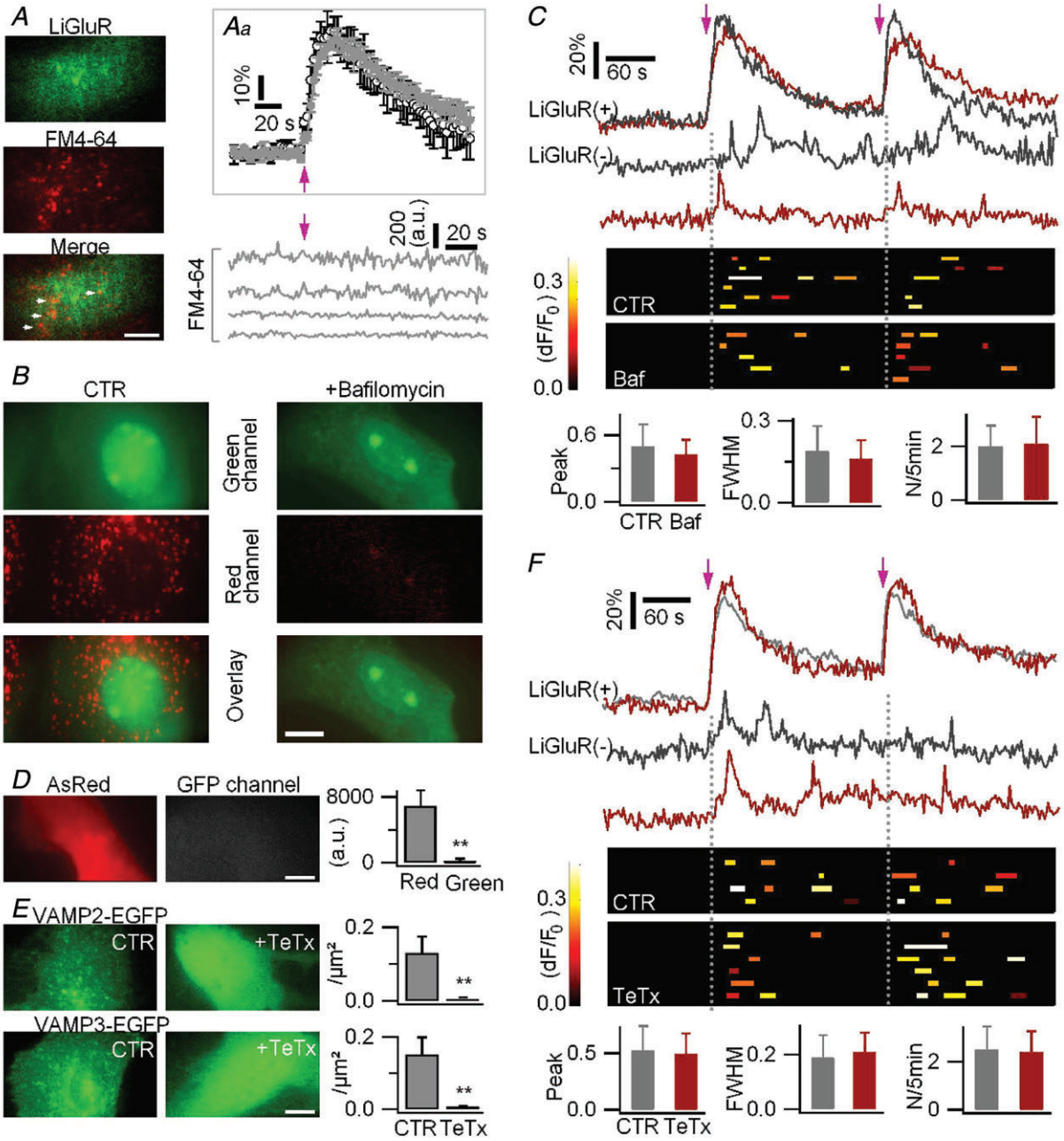


**Figure 6. Exocytosis is not the pathway for LiGluR-evoked glutamate release by astrocytes**
*A*, astrocytes were transfected with LiGluR-GFP and loaded with the red-fluorescent lysosomal marker FM4–64. Inset (*Aa*) average LiGluR-evoked $Ca^{2+}$ rises were similar in control (black trace) and FM4–64-loaded cells (grey trace; $n = 6$ trials, 3 cells for each). Bottom right, fluorescence intensity of the FM6–64 loaded lysosomal vesicles was unchanged upon LiGluR photoactivation. *B*, inhibition of V-ATPase activity by bafilomycin A1 (100 nM, 1 h) abolished the vesicular accumulation (red channel, epifluorescence) of acridine orange (15 $\mu$M, 15 min). *C*, LiGluR-evoked $Ca^{2+}$ rises in LiGluR(−) astrocytes were unchanged in cells treated with bafilomycin (Baf) for 1 h. Astrocytes were co-transfected with LiGluR–RFP and AsRed, and loaded with Fluo-4 AM. Top, sample traces (grey, control; red, bafilomycin). Middle, summary plots of the LiGluR-evoked $Ca^{2+}$ events in LiGluR(−) cells. Bottom, the relative peak amplitude, FWHM, and frequency (N/5 min) of the $Ca^{2+}$ transients (16 events, 6 cells in control; 14 events, 5 cells in bafilomycin, $P > 0.39$). *D*, transfection of TeTx in astrocytes did not affect the GFP imaging channel. Right, fluorescence counts in red and green channels, respectively ($n = 10$ cells). AsRed was co-transfected to localize the transfected cell. *E*, transfection of TeTx in astrocytes abolished the vesicular targeting of VAMP2-EGFP and VAMP3-EGFP. Right, puncta density ($n = 16$–19 cells for each). *F*, LiGluR-evoked near-membrane $Ca^{2+}$ transients in LiGluR(−) cells were unchanged in astrocytes co-transfected with TeTx (grey, control, 15 events, 4 cells; red, TeTx, 19 events, 6 cells; $P > 0.32$). Bars, 10 $\mu$m.

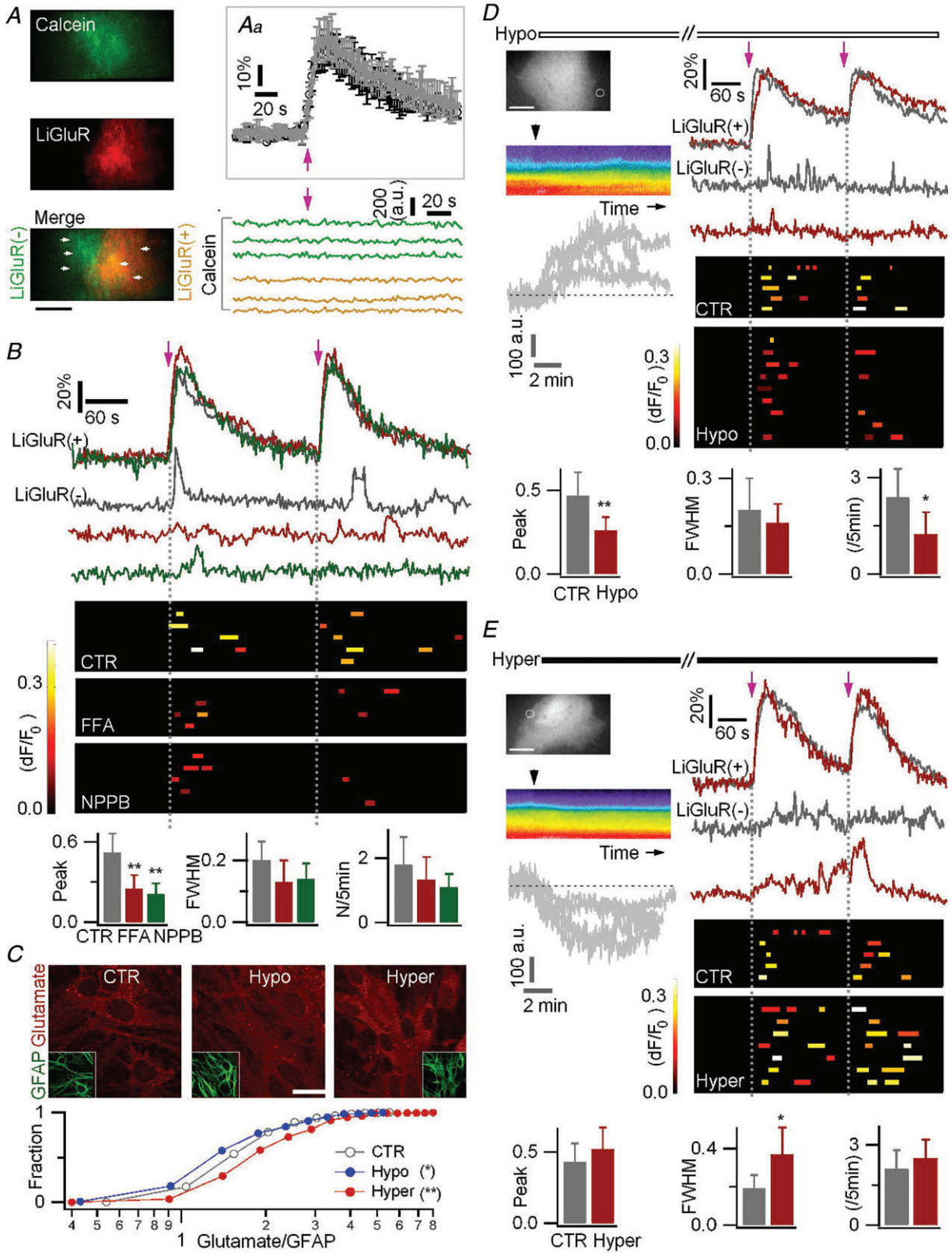


**Figure 7. An anion channel mediates LiGluR-evoked glutamate release by astrocytes**
*A*, astrocytes were co-transfected with LiGluR-RFP and AsRed, and loaded with calcein AM. Inset (*Aa*), similar LiGluR-evoked $Ca^{2+}$ rises in LiGluR(+) astrocytes in the absence (average black trace, $n = 6$) and in the presence of calcein (average grey trace, $n = 6$). Bottom, LiGluR photoactivation (arrow) left the calcein fluorescence stable

submit simultaneously the astrocytes to osmotic shock and LiGluR photoactivation. However, we argued that if LiGluR-evoked glutamate release involves a channel, osmotic shocks should change the amount of glutamate available for release. Using immunostaining (Gorg *et al.* 2010), we first confirmed that a 20 min treatment with hypotonic (−17%) solution led to a reduction of intracellular glutamate content, an opposite effect being induced by hypertonic (+23%) solution (Fig. 7*C*). We estimated the LiGluR-evoked astrocyte-to-astrocyte communication in cells challenged by a change of osmotic pressure, when osmotically altered $Ca^{2+}$ levels had stabilized, and the LiGluR-evoked $Ca^{2+}$ rise in LiGluR(+) cells were normal (Supplemental Table 2). Interestingly, the LiGluR-evoked $Ca^{2+}$ transients in LiGluR(−) astrocytes were reduced by the hypotonic solution treatment (Fig. 7*D*), and enhanced by the hypertonic solution treatment (Fig. 7*E*), as expected if release occurs by efflux of glutamate from the cytosol. Altogether, these results suggest that LiGluR-evoked glutamate release involves a glutamate-permeable anion channel.

## Discussion

Here, we show that photoactivation of the light-gated $Ca^{2+}$-permeable channels, LiGluR and CatCh, unlike ChR2, evokes $Ca^{2+}$ signals in cultured cortical astrocytes. Using evanescent-field excitation for near-membrane $Ca^{2+}$ imaging and epifluorescence for LiGluR activation and inactivation, we could precisely and reliably control the amplitude and duration of the LiGluR-evoked $Ca^{2+}$ rise. We also show that the photoactivation of LiGluR triggered astrocyte-to-astrocyte communication due to anion channel-mediated glutamate release. These results demonstrate the power of LiGluR, in association with all-optical tools, to control $Ca^{2+}$ activity and to monitor downstream events in electrically silent cells. Finally, the light activation with genetically encoded proteins holds the promise for a specific remote control of astrocyte activity *in situ*.

Low-intensity ($0.3\ mW\ mm^{-2}$ for tens of milliseconds) light pulses reliably trigger $Ca^{2+}$ rise in astrocytes expressing LiGluR. The CatCh photoactivation could also induce $Ca^{2+}$ rise, although it required an order of magnitude more power and longer illumination ($15.1\ mW\ mm^{-2}$, 1 s), and unlike the stable LiGluR-evoked responses, the CatCh-evoked responses faded in amplitude upon repeated stimulation. Unlike LiGluR and CatCh, ChR2(H134R), even using pulses of higher intensity ($27.3\ mW\ mm^{-2}$, up to 1 s), which activate neurons, failed to evoke substantial $Ca^{2+}$ rise in astrocytes. In line with a previous study (Zhang & Oertner, 2007), we found that in neurons, the ChR2-evoked $Ca^{2+}$ transients are mostly due to the secondary activation of VGCCs. In astrocytes we found that ChR2 photoactivation is unable to generate secondary $Ca^{2+}$ since astrocytes have low input resistance and express little VGCCs (Verkhratsky & Steinhäuser, 2000). Hence, the inability of ChR2 to evoke reliable $Ca^{2+}$ signals in astrocytes results probably from its relatively weak $Ca^{2+}$ permeability. Previous work in oocytes showed that ChR2 behaves as a $Ca^{2+}$ permeable channel; however the experiments were conducted in elevated 80 mM $Ca^{2+}$, and the current measured in the presence of BAPTA to inactivate a $Ca^{2+}$-sensitive chloride current was much smaller than the current measured in 110 mM $Na^{+}$ (Nagel *et al.* 2003). Moreover, lowering the external $Ca^{2+}$ concentration from 80 mM to 20 mM or 2 mM made the ChR2-gated $Ca^{2+}$ rises in HEK cells much reduced and less reliable (Lin *et al.* 2009). Finally, the relative $Ca^{2+}$ permeability of ChR2 ($P_{Ca}/P_{Na}$ ~0.12) estimated in 20 mM $Ca^{2+}$ (Lin *et al.* 2009) is relatively weak, in comparison with LiGluR ($P_{Ca}/P_{mono}$ ~1.2) (Egebjerg & Heinemann, 1993) and CatCh ($P_{Ca}/P_{Na}$ ~0.24) (Kleinlogel *et al.* 2011). The ChR2 is mainly permeable to $H^{+}$ ($P_{H}/P_{Na}$ ~$1.06 \times 10^{6}$)

in the ROIs (left panel, arrowhead, 2 $\mu$m × 2 $\mu$m) in LiGluR(+) cells (green traces) and LiGluR(−) cells (yellow traces). Bar, 5 $\mu$m. *B*, astrocytes were co-transfected with LiGluR-RFP and AsRed, and loaded with Fluo-4 AM. The LiGluR-evoked $Ca^{2+}$ transients in LiGluR(−) astrocytes were reduced by the anion channel blockers, flufenamic acid (FFA, 50 $\mu$M, red) and 5-nitro-2-(3-phenylpropylamino) benzoic acid (NPPB, 100 $\mu$M, green). Control (CTR, grey traces, 12 events, 5 cells). FFA (red traces, 7 events, 4 cells). NPPB (green traces, 7 events, 5 cells. *C*, astrocytes were immunostained with glutamate (red) and GFAP (green) antibodies, and the glutamate/GFAP fluorescence intensity ratio was plotted as a cumulative histogram. Intracellular glutamate immunostaining was altered by 20 min treatment of hypo- (blue) or hyper-tonic solutions (red) ($n = 244$–606 regions from 3 trials for each condition, KS test). Bar, 10 $\mu$m. *D*–*E*, effect of hypo-osmotic (−25 mM NaCl) and hyper-osmotic (+50 mM sucrose; 15–20 min) solutions on LiGluR-evoked $Ca^{2+}$ transients in LiGluR(−) astrocytes co-transfected with LiGluR-RFP and AsRed, and loaded with Fluo-4 AM. Left, pseudocolour kymographs show the transient cell swelling or shrinking, respectively, following the change of osmotic pressure (black arrowhead, application time) on GFP-expressing astrocytes. The same result is obtained when plotting the fluorescence change in ROIs lining the outer/inner side of the cell border (grey traces, $n = 4$ cells each). Right, sample traces and summary plots of LiGluR-evoked $Ca^{2+}$ transients in LiGluR(−) astrocytes. Bottom, statistical comparison of LiGluR-evoked $Ca^{2+}$ transients in control (CTR, 14 events, 5 cells), hypotonic (Hypo, 16 events, 9 cells), and hypertonic (Hyper, 23 events, 7 cells) solutions. Bars, 10 $\mu$m.

(Nagel *et al.* 2003; Lin *et al.* 2009), as confirmed in our $H^+$-GFP quenching experiments. The LiGluR-mediated $Ca^{2+}$ rises we have seen in cultured cortical astrocytes are reliable and temporally well controlled. This contrasts with the variable ChR2-gated $Ca^{2+}$ signals seen in brainstem astrocytes, which require long-lasting (tens of seconds) illumination (Gourine *et al.* 2010). The differences between our observations and those of Gourine *et al.* could be attributed to their longer illumination and to specialized features of their brainstem astrocytes that responded with a $Ca^{2+}$ rise to a gentle acidification (pH 7.4 to 7.2), a feature not found for cortical astrocytes (Gourine *et al.* 2010). Interestingly, CatCh-evoked $Ca^{2+}$ signals, like near-membrane spontaneous $Ca^{2+}$ events (Shigetomi *et al.* 2010), depend only on the $Ca^{2+}$ influx. In contrast, LiGluR-evoked signals, like near-membrane ATP-evoked events (Shigetomi *et al.* 2010), involve both $Ca^{2+}$ influx and $Ca^{2+}$ stores. Our results indicate LiGluR and CatCh as useful tools to investigate $Ca^{2+}$-regulated cellular responses in astrocytes and possibly in other non-excitable cells.

Astrocytes in culture release gliotransmitters in a $Ca^{2+}$-dependent manner which shares similarities with astrocyte-to-neuron communication *in situ* (Halassa & Haydon, 2010). The first demonstration of exocytosis by small synaptic-like vesicle carrying a vesicular glutamate transporter came from cultured astrocytes (Bezzi *et al.* 2004), and therefore, although astrocytes in culture differ from their *in situ* counterparts (Cahoy *et al.* 2008), they stand as a good model to establish new tools and to study the cellular and molecular mechanisms of gliotransmitter release. Here we show that the LiGluR-evoked $Ca^{2+}$ rises evoke $Ca^{2+}$ transients in adjacent LiGluR(−) astrocytes which are consistent with a chemical transmission between LiGluR(+) and LiGluR(−) astrocytes. Unlike the stereotyped light-gated $Ca^{2+}$ rises in LiGluR(+) astrocytes, the $Ca^{2+}$ transients in LiGluR(−) cells have a small amplitude, relatively short duration, and, unlike the glutamate-evoked Ref-Ca responses, a variable latency probably due to a sluggish coupling between the $Ca^{2+}$ rise and the activation of the release pathway in LiGluR(+) cells. Combining pharmacological dissections with the all-optical investigation, we show that LiGluR photoactivation induces glutamate release to activate mGluR receptor in neighbouring astrocytes.

Among the mechanisms of glutamate release by astrocytes, a fast $Ca^{2+}$-regulated exocytosis which shares features with neurotransmitter release was proposed as a major pathway (Bezzi *et al.* 2004; Hamilton & Attwell, 2010; Parpura *et al.* 2011). Nonetheless, we showed that astrocytes handle the exo/endo-cytotic marker FM4–64 differently from neurons (Li *et al.* 2009), and that mechanical stimulation triggers asynchronous $Ca^{2+}$-dependant exocytosis of sialin-positive lysosomes (Li *et al.* 2008). Here we show that LiGluR photoactivation triggers astrocyte-to-astrocyte communication which operates on a slow time base, is insensitive to blockers of vesicular release, bafilomycin and TeTx (Hamilton & Attwell, 2010), and does not induce FM4–64-labelled lysosomal exocytosis. These results indicate that the exocytosis of neither small synaptic-like vesicles nor lysosomes is involved in LiGluR-evoked glutamate release from astrocytes in culture.

Using hemichannel and glutamate transporter blockers, we also exclude hemichannels and glutamate transporters as possible pathways for LiGluR-evoked glutamate release. Our experiments using anion channel blockers and treatments with hypo/hypertonic solutions suggest anion channels as the pathway for the LiGluR-gated glutamate release. Glutamate-permeable channels in astrocytes include volume-regulated anion channels and $Ca^{2+}$-activated chloride channels (Takano *et al.* 2005; Kimelberg *et al.* 2006; Park *et al.* 2009). Identifying among the cloned channels (Duran *et al.* 2010) the channel that mediates the LiGluR-evoked glutamate release will require new experiments.

The LiGluR-evoked astrocyte-to-astrocyte communication needs relatively long lasting $Ca^{2+}$ rises, raising the question of the functional significance of our results. Similar $Ca^{2+}$ signals were observed *in situ* in conditions such as Alzheimer's disease (Kuchibhotla *et al.* 2009), epilepsy (Ding *et al.* 2007; Gomez-Gonzalo *et al.* 2010), and NMDA receptor-mediated slow inward currents (SICs) (Fellin *et al.* 2004; Shigetomi *et al.* 2008). LiGluR-evoked $Ca^{2+}$ rises that mimic the response to a physiological application of glutamate failed to evoke glutamate-mediated astrocyte-to-astrocyte communication. More experiments *in situ* will be needed to clarify whether astrocyte glutamate release is relevant mainly to pathological conditions, or whether smaller $Ca^{2+}$ transients evoked by LiGluR in the very thin astrocytic processes present *in situ* will be sufficient to mediate astrocyte-to-astrocyte and astrocyte-to-neuron communications in physiological conditions.

The opsins offer the advantage of working without introduction of the photochrome. This makes them easier to use but the lack of efficacy and reproducibility to activate astrocytes can be a problem since it might require toxic levels of light. The light intensity used to induce $Ca^{2+}$ rise in astrocytes with ChR2 (Gourine *et al.* 2010) might induce a local change in temperature of the order of $\sim 5^{\circ}$C according to the quantitative estimation made by Yizhar *et al.* (2011). Since the MAG photoswitch can be introduced to LiGluR *in vivo* as shown in the zebrafish spinal cord and the mouse eye (Szobota *et al.* 2007; Wyart *et al.* 2009; Caporale *et al.* 2011), and the LiGuR-mediated $Ca^{2+}$ elevation requires low light intensity, LiGluR appears as a better tool than the ChR2 to use for the astrocytes *in situ*.

In conclusion, we show that the $Ca^{2+}$-permeable LiGluR and CatCh extend our repertoire of tools to control astrocyte activity and to study downstream cellular events regulated by $Ca^{2+}$ elevation. Opsin-derived proteins and LiGluR-based approaches control very efficiently neuronal activity *in vitro* and *in situ* (Janovjak *et al.* 2010; Szobota & Isacoff, 2010; Fenno *et al.* 2011). Our results in the present study show that LiGluR allows us not only to efficiently shape the $Ca^{2+}$ elevations, but also to image the $Ca^{2+}$ activity of electrically silent cells using highly sensitive TIRFM, allowing a better understanding of astrocytic signalling.

## References


Agulhon C, Fiacco TA & McCarthy KD (2010). Hippocampal short- and long-term plasticity are not modulated by astrocyte $Ca^{2+}$ signaling. *Science* **327**, 1250–1254.

Agulhon C, Petravicz J, McMullen AB, Sweger EJ, Minton SK, Taves SR, Casper KB, Fiacco TA & McCarthy KD (2008). What is the role of astrocyte calcium in neurophysiology? *Neuron* **59**, 932–946.

Andersson M & Hanse E (2010). Astrocytes impose postburst depression of release probability at hippocampal glutamate synapses. *J Neurosci* **30**, 5776–5780.

Angulo MC, Kozlov AS, Charpak S & Audinat E (2004). Glutamate released from glial cells synchronizes neuronal activity in the hippocampus. *J Neurosci* **24**, 6920–6927.

Benfenati V, Caprini M, Dovizio M, Mylonakou MN, Ferroni S, Ottersen OP & Amiry-Moghaddam M (2011). An aquaporin-4/transient receptor potential vanilloid 4 (AQP4/TRPV4) complex is essential for cell-volume control in astrocytes. *Proc Natl Acad Sci U S A* **108**, 2563–2568.

Bezzi P, Gundersen V, Galbete JL, Seifert G, Steinhauser C, Pilati E & Volterra A (2004). Astrocytes contain a vesicular compartment that is competent for regulated exocytosis of glutamate. *Nat Neurosci* **7**, 613–620.

Bowman EJ, Siebers A & Altendorf K (1988). Bafilomycins: a class of inhibitors of membrane ATPases from microorganisms, animal cells, and plant cells. *Proc Natl Acad Sci U S A* **85**, 7972–7976.

Bowser DN & Khakh BS (2007). Vesicular ATP is the predominant cause of intercellular calcium waves in astrocytes. *J Gen Physiol* **129**, 485–491.

Cahoy JD, Emery B, Kaushal A, Foo LC, Zamanian JL, Christopherson KS, Xing Y, Lubischer JL, Krieg PA, Krupenko SA, Thompson WJ & Barres BA (2008). A transcriptome database for astrocytes, neurons, and oligodendrocytes: a new resource for understanding brain development and function. *J Neurosci* **28**, 264–278.

Cai Z, Schools GP & Kimelberg HK (2000). Metabotropic glutamate receptors in acutely isolated hippocampal astrocytes: developmental changes of mGluR5 mRNA and functional expression. *Glia* **29**, 70–80.

Caporale N, Kolstad KD, Lee T, Tochitsky I, Dalkara D, Trauner D, Kramer R, Dan Y, Isacoff EY & Flannery JG (2011). LiGluR restores visual responses in rodent models of inherited blindness. *Mol Ther* **19**, 1212–1219

Demuro A & Parker I (2005). "Optical patch-clamping": single-channel recording by imaging $Ca^{2+}$ flux through individual muscle acetylcholine receptor channels. *J Gen Physiol* **126**, 179–192.

Ding S, Fellin T, Zhu Y, Lee SY, Auberson YP, Meaney DF, Coulter DA, Carmignoto G & Haydon PG (2007). Enhanced astrocytic $Ca^{2+}$ signals contribute to neuronal excitotoxicity after status epilepticus. *J Neurosci* **27**, 10674–10684.

Duran C, Thompson CH, Xiao Q & Hartzell HC (2010). Chloride channels: often enigmatic, rarely predictable. *Annu Rev Physiol* **72**, 95–121.

Dzubay JA & Jahr CE (1999). The concentration of synaptically released glutamate outside of the climbing fiber-Purkinje cell synaptic cleft. *J Neurosci* **19**, 5265–5274.

Egebjerg J & Heinemann SF (1993). $Ca^{2+}$ permeability of unedited and edited versions of the kainate selective glutamate receptor GluR6. *Proc Natl Acad Sci U S A* **90**, 755–759.

Fam SR, Gallagher CJ & Salter MW (2000). $P2Y_1$ purinoceptor-mediated $Ca^{2+}$ signaling and $Ca^{2+}$ wave propagation in dorsal spinal cord astrocytes. *J Neurosci* **20**, 2800–2808.

Fellin T, Pascual O, Gobbo S, Pozzan T, Haydon PG & Carmignoto G (2004). Neuronal synchrony mediated by astrocytic glutamate through activation of extrasynaptic NMDA receptors. *Neuron* **43**, 729–743.

Fenno L, Yizhar O & Deisseroth K (2011). The development and application of optogenetics. *Annu Rev Neurosci* **34**, 389–412.

Fiacco TA, Agulhon C & McCarthy KD (2009). Sorting out astrocyte physiology from pharmacology. *Annu Rev Pharmacol Toxicol* **49**, 151–174.

Fiacco TA, Agulhon C, Taves SR, Petravicz J, Casper KB, Dong X, Chen J & McCarthy KD (2007). Selective stimulation of astrocyte calcium in situ does not affect neuronal excitatory synaptic activity. *Neuron* **54**, 611–626.

Frank S, Gaume B, Bergmann-Leitner ES, Leitner WW, Robert EG, Catez F, Smith CL & Youle RJ (2001). The role of dynamin-related protein 1, a mediator of mitochondrial fission, in apoptosis. *Dev Cell* **1**, 515–525.

Gomez-Gonzalo M, Losi G, Chiavegato A, Zonta M, Cammarota M, Brondi M, Vetri F, Uva L, Pozzan T, de Curtis M, Ratto GM & Carmignoto G (2010). An excitatory loop with astrocytes contributes to drive neurons to seizure threshold. *PLoS Biol* **8**, e1000352.

Gordon GR, Iremonger KJ, Kantevari S, Ellis-Davies GC, MacVicar BA & Bains JS (2009). Astrocyte-mediated distributed plasticity at hypothalamic glutamate synapses. *Neuron* **64**, 391–403.

Gorg B, Morwinsky A, Keitel V, Qvartskhava N, Schror K & Haussinger D (2010). Ammonia triggers exocytotic release of L-glutamate from cultured rat astrocytes. *Glia* **58**, 691–705.

Gorostiza P, Volgraf M, Numano R, Szobota S, Trauner D & Isacoff EY (2007). Mechanisms of photoswitch conjugation and light activation of an ionotropic glutamate receptor. *Proc Natl Acad Sci U S A* **104**, 10865–10870.

Gourine AV, Kasymov V, Marina N, Tang F, Figueiredo MF, Lane S, Teschemacher AG, Spyer KM, Deisseroth K & Kasparov S (2010). Astrocytes control breathing through pH-dependent release of ATP. *Science* **329**, 571–575.

Gradinaru V, Mogri M, Thompson KR, Henderson JM & Deisseroth K (2009). Optical deconstruction of parkinsonian neural circuitry. *Science* **324**, 354–359.

Halassa MM & Haydon PG (2010). Integrated brain circuits: astrocytic networks modulate neuronal activity and behavior. *Annu Rev Physiol* **72**, 335–355.

Hamilton NB & Attwell D (2010). Do astrocytes really exocytose neurotransmitters? *Nat Rev Neurosci* **11**, 227–238.

Janovjak H, Szobota S, Wyart C, Trauner D & Isacoff EY (2010). A light-gated, potassium-selective glutamate receptor for the optical inhibition of neuronal firing. *Nat Neurosci* **13**, 1027–1032.

Kimelberg HK, Macvicar BA & Sontheimer H (2006). Anion channels in astrocytes: biophysics, pharmacology, and function. *Glia* **54**, 747–757.

Kleinlogel S, Feldbauer K, Dempski RE, Fotis H, Wood PG, Bamann C & Bamberg E (2011). Ultra light-sensitive and fast neuronal activation with the $Ca^{2+}$-permeable channelrhodopsin CatCh. *Nat Neurosci* **14**, 513–518.

Kuchibhotla KV, Lattarulo CR, Hyman BT & Bacskai BJ (2009). Synchronous hyperactivity and intercellular calcium waves in astrocytes in Alzheimer mice. *Science* **323**, 1211–1215.

Li D, Hérault K, Oheim M & Ropert N (2009). FM dyes enter via a store-operated calcium channel and modify calcium signaling of cultured astrocytes. *Proc Natl Acad Sci U S A* **106**, 21960–21965.

Li D, Ropert N, Koulakoff A, Giaume C & Oheim M (2008). Lysosomes are the major vesicular compartment undergoing $Ca^{2+}$-regulated exocytosis from cortical astrocytes. *J Neurosci* **28**, 7648–7658.

Lin JY, Lin MZ, Steinbach P & Tsien RY (2009). Characterization of engineered channelrhodopsin variants with improved properties and kinetics. *Biophys J* **96**, 1803–1814.

McMahon HT, Ushkaryov YA, Edelmann L, Link E, Binz T, Niemann H, Jahn R & Sudhof TC (1993). Cellubrevin is a ubiquitous tetanus-toxin substrate homologous to a putative synaptic vesicle fusion protein. *Nature* **364**, 346–349.

Miyaji T, Echigo N, Hiasa M, Senoh S, Omote H & Moriyama Y (2008). Identification of a vesicular aspartate transporter. *Proc Natl Acad Sci U S A* **105**, 11720–11724.

Nadrigny F, Li D, Kemnitz K, Ropert N, Koulakoff A, Rudolph S, Vitali M, Giaume C, Kirchhoff F & Oheim M (2007). Systematic colocalization errors between acridine orange and EGFP in astrocyte vesicular organelles. *Biophys J* **93**, 969–980.

Nadrigny F, Rivals I, Hirrlinger PG, Koulakoff A, Personnaz L, Vernet M, Allioux M, Chaumeil M, Ropert N, Giaume C, Kirchhoff F & Oheim M (2006). Detecting fluorescent protein expression and co-localisation on single secretory vesicles with linear spectral unmixing. *Eur Biophys J* **35**, 533–547.

Nagel G, Brauner M, Liewald JF, Adeishvili N, Bamberg E & Gottschalk A (2005). Light activation of channelrhodopsin-2 in excitable cells of *Caenorhabditis elegans* triggers rapid behavioral responses. *Curr Biol* **15**, 2279–2284.

Nagel G, Szellas T, Huhn W, Kateriya S, Adeishvili N, Berthold P, Ollig D, Hegemann P & Bamberg E (2003). Channelrhodopsin-2, a directly light-gated cation-selective membrane channel. *Proc Natl Acad Sci U S A* **100**, 13940–13945.

Nakashima S, Hiraku Y, Tada-Oikawa S, Hishita T, Gabazza EC, Tamaki S, Imoto I, Adachi Y & Kawanishi S (2003). Vacuolar $H^+$-ATPase inhibitor induces apoptosis via lysosomal dysfunction in the human gastric cancer cell line MKN-1. *J Biochem* **134**, 359–364.

Numano R, Szobota S, Lau AY, Gorostiza P, Volgraf M, Roux B, Trauner D & Isacoff EY (2009). Nanosculpting reversed wavelength sensitivity into a photoswitchable iGluR. *Proc Natl Acad Sci U S A* **106**, 6814–6819.

Park H, Oh SJ, Han KS, Woo DH, Mannaioni G, Traynelis SF & Lee CJ (2009). Bestrophin-1 encodes for the $Ca^{2+}$-activated anion channel in hippocampal astrocytes. *J Neurosci* **29**, 13063–13073.

Parpura V, Grubisic V & Verkhratsky A (2011). $Ca^{2+}$ sources for the exocytotic release of glutamate from astrocytes. *Biochim Biophys Acta* **1813**, 984–991.

Perea G & Araque A (2007). Astrocytes potentiate transmitter release at single hippocampal synapses. *Science* **317**, 1083–1086.

Rossi DJ, Oshima T & Attwell D (2000). Glutamate release in severe brain ischaemia is mainly by reversed uptake. *Nature* **403**, 316–321.

Sasaki T, Kuga N, Namiki S, Matsuki N & Ikegaya Y (2011). Locally synchronized astrocytes. *Cereb Cortex* **21**, 1889–1900.

Scemes E & Giaume C (2006). Astrocyte calcium waves: what they are and what they do. *Glia* **54**, 716–725.

Shigetomi E, Bowser DN, Sofroniew MV & Khakh BS (2008). Two forms of astrocyte calcium excitability have distinct effects on NMDA receptor-mediated slow inward currents in pyramidal neurons. *J Neurosci* **28**, 6659–6663.

Shigetomi E, Kracun S, Sofroniew MV & Khakh BS (2010). A genetically targeted optical sensor to monitor calcium signals in astrocyte processes. *Nat Neurosci* **13**, 759–766.

Stout CE, Costantin JL, Naus CC & Charles AC (2002). Intercellular calcium signaling in astrocytes via ATP release through connexin hemichannels. *J Biol Chem* **277**, 10482–10488.

Szobota S & Isacoff EY (2010). Optical control of neuronal activity. *Annu Rev Biophys* **39**, 329–348.

Szobota S, Gorostiza P, Del Bene F, Wyart C, Fortin DL, Kolstad KD, Tulyathan O, Volgraf M, Numano R, Aaron HL, Scott EK, Kramer RH, Flannery J, Baier H, Trauner D & Isacoff EY (2007). Remote control of neuronal activity with a light-gated glutamate receptor. *Neuron* **54**, 535–545.

Takano T, Kang J, Jaiswal JK, Simon SM, Lin JH, Yu Y, Li Y, Yang J, Dienel G, Zielke HR & Nedergaard M (2005). Receptor-mediated glutamate release from volume sensitive channels in astrocytes. *Proc Natl Acad Sci U S A* **102**, 16466–16471.

Thompson RJ, Zhou N & MacVicar BA (2006). Ischemia opens neuronal gap junction hemichannels. *Science* **312**, 924–927.

Verkhratsky A & Steinhäuser C (2000). Ion channels in glial cells. *Brain Res Brain Res Rev* **32**, 380–412.

Volgraf M, Gorostiza P, Numano R, Kramer RH, Isacoff EY & Trauner D (2006). Allosteric control of an ionotropic glutamate receptor with an optical switch. *Nat Chem Biol* **2**, 47–52.

Wang X, Lou N, Xu Q, Tian GF, Peng WG, Han X, Kang J, Takano T & Nedergaard M (2006). Astrocytic $Ca^{2+}$ signaling evoked by sensory stimulation in vivo. *Nat Neurosci* **9**, 816–823.

Wyart C, Del Bene F, Warp E, Scott EK, Trauner D, Baier H & Isacoff EY (2009). Optogenetic dissection of a behavioural module in the vertebrate spinal cord. *Nature* **461**, 407–410.

Yizhar O, Fenno LE, Davidson TJ, Mogri M & Deisseroth K (2011). Optogenetics in neural systems. *Neuron* **71**, 9–34.

Ye ZC, Wyeth MS, Baltan-Tekkok S & Ransom BR (2003). Functional hemichannels in astrocytes: a novel mechanism of glutamate release. *J Neurosci* **23**, 3588–3596.

Zhang YP & Oertner TG (2007). Optical induction of synaptic plasticity using a light-sensitive channel. *Nat Methods* **4**, 139–141.

Zhang Z, Chen G, Zhou W, Song A, Xu T, Luo Q, Wang W, Gu XS & Duan S (2007). Regulated ATP release from astrocytes through lysosome exocytosis. *Nat Cell Biol* **9**, 945–953.

Zhou Q, Petersen CC & Nicoll RA (2000). Effects of reduced vesicular filling on synaptic transmission in rat hippocampal neurones. *J Physiol* **525**, 195–206.

## Author contributions

D.L., E.Y.I., M.O. and N.R. designed the research; K.H. prepared cell culture and performed the fluorescence immunostaining; D.L. performed the experiments and analysed the data; D.L., E.Y.I., M.O. and N.R. wrote the manuscript. Experiments were done at Paris Descartes university. All authors have approved the final version for publication.

## Acknowledgements

We thank Patrice Jegouzo for technical support, Florent Jean for administrative assistance, Ernst Bamberg (MPI für Biophysik, Frankfurt, Germany) for the CatCh-YFP plasmid. We also thank Etienne Audinat for discussion and comments of an earlier version of the manuscript. Confocal imaging was performed at the Paris Descartes imaging plateform. The work was supported by the European Union (FP6-STRP no. 037897-AUTOSCREEN, FP7-ERA-NET no. 006-03-NANOSYN), and the Agence Nationale de la Recherche (ANR PNANO 05-051, ANR P3N 09-044-02). D.L. acknowledges post-doctoral funding from Ecole des Neurosciences de Paris Ile-de-France (ENP), EU and ANR. E.Y.I. received funding from the National Institutes of Health Nanomedicine Development Center for the Optical Control of Biological Function (PN2EY018241) and the ENP sabbatical programme.